

EX7/3



Progress of High-Performance Steady-State Plasma and Critical PWI Issues in the LHD

H. Kasahara, M. Tokitani, Y. Yoshimura, K. Nagasaki¹, N. Ashikawa, Y. Ueda², G. Motojima, M. Shoji, T. Seki, K. Saito, R. Seki, S. Kamio, G. Nomura, G. Nomura, F. Shimpo, S. Kubo, T. Shimosuma, H. Igami, H. Takahashi, S. Itoh, T. Ii, S. Masuzaki, H. Tanaka, J. Miyazawa, H. Tsuchiya, N. Tamura, T. Tokuzawa, N. Yoshida³, T. Shinya⁴, Y. P. Zhao⁵, J. G. Kwak⁶, T. Mutoh, and LHD Experiment Group

National Institute for Fusion Science

¹Kyoto University, ²Osaka University, ³Kyushu University,

⁴University of Tokyo, ⁵ASIPP, ⁶NFRI

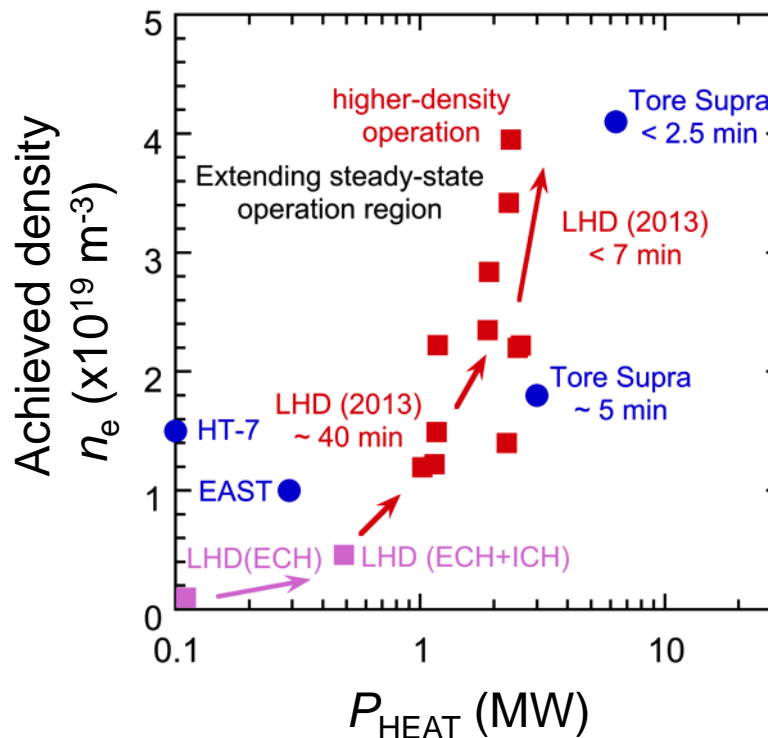
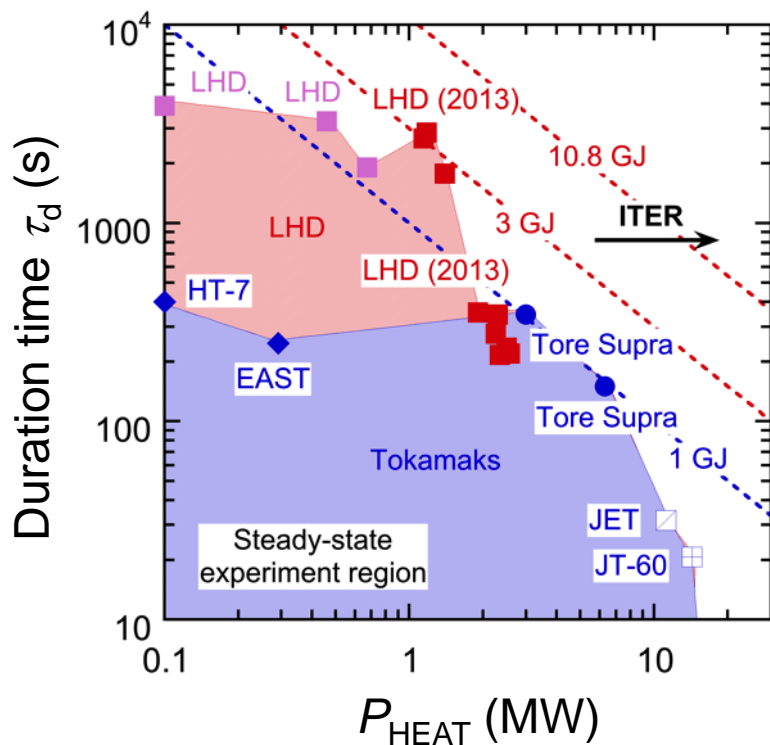


- *The extension of steady-state plasma duration with MW-class heating, and the operation regions*
- *Result of ultra-long pulse plasma duration with $\tau_d \sim 48$ min, $P_{RF} \sim 1.2$ MW, $n_e \sim 1.2 \times 10^{19} \text{ m}^{-3}$, $T_e \sim T_i \sim 2$ keV, and $W_{inj} \sim 3.4$ GJ*
 - *Thermal behavior and typical temperatures*
 - Inhomogeneity of divertor heat flux*
 - *The steady-state was terminated by sudden unintended entrance of the exfoliated mixed-material layers (MMLs) with continuous divertor erosion*
 - *Characteristics of the MMLs*
 - Thick region, the growth rate, the main elements, the physical property, and the trappable ability of He particles*
 - *Preliminary estimation of He particle balance with the MMLs*
- *Summary and future plans*



- *The extension of steady-state plasma duration with MW-class heating, and the operation regions*
- *Result of ultra-long pulse plasma duration with $\tau_d \sim 48$ min, $P_{RF} \sim 1.2$ MW, $n_e \sim 1.2 \times 10^{19} \text{ m}^{-3}$, $T_e \sim T_i \sim 2$ keV, and $W_{inj} \sim 3.4$ GJ*
 - *Thermal behavior and typical temperatures*
Inhomogeneity of divertor heat flux
 - *The steady-state was terminated by sudden unintended entrance of the exfoliated mixed-material layers (MMLs) with continuous divertor erosion*
 - *Characteristics of the MMLs*
Thick region, the growth rate, the main elements, the physical property, and the trappable ability of He particles
 - *Preliminary estimation of He particle balance with the MMLs*
- *Summary and future plans*

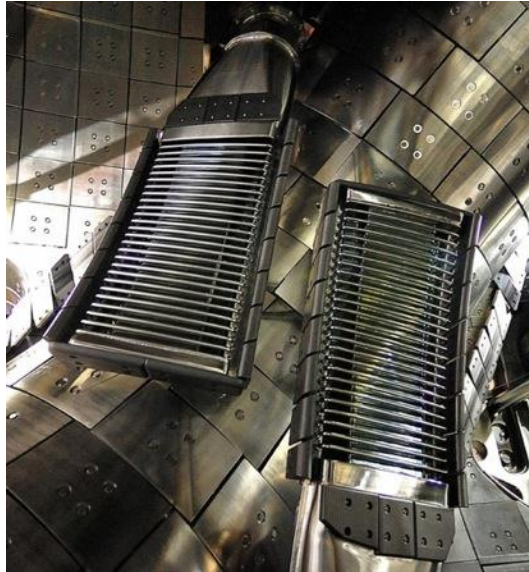
Extending the high-power and high-performance steady-state operation region



In 2013, there were two remarkable extensions of SSO

- Ultra-long pulse plasma (~ 48 min, 1MW-class)
 $1.2 \times 10^{19} \text{m}^{-3}$, 2keV, 2859s@1.2MW(ECH+ICH), 3.36GJ
- Higher power long-pulse plasma (> 200 sec, 2MW-class)
 $3.3 \times 10^{19} \text{m}^{-3}$, 1.5keV, 345s@2.3MW(ECH+ICH)

Development of high-power heating systems, and the integration and optimizing of plasma operations



HAS antenna (#3.5 port)
Field-aligned, large wavenumber
 $\eta_{\text{heat}} \sim 90\%$, $S_{\text{excite}} \sim 0.27 \text{ m}^2$



FAIT antenna (#4.5)
Field-aligned, transforming
 $\eta_{\text{heat}} \sim 80\%$, $S_{\text{excite}} \sim 0.12 \text{ m}^2$



PA antenna (#7.5)
Large antenna coupling
w/o FS ($\eta_{\text{heat}} \sim 60\%$)
(upper strap)
w FS ($\eta_{\text{heat}} 70\%$)
(lower strap)

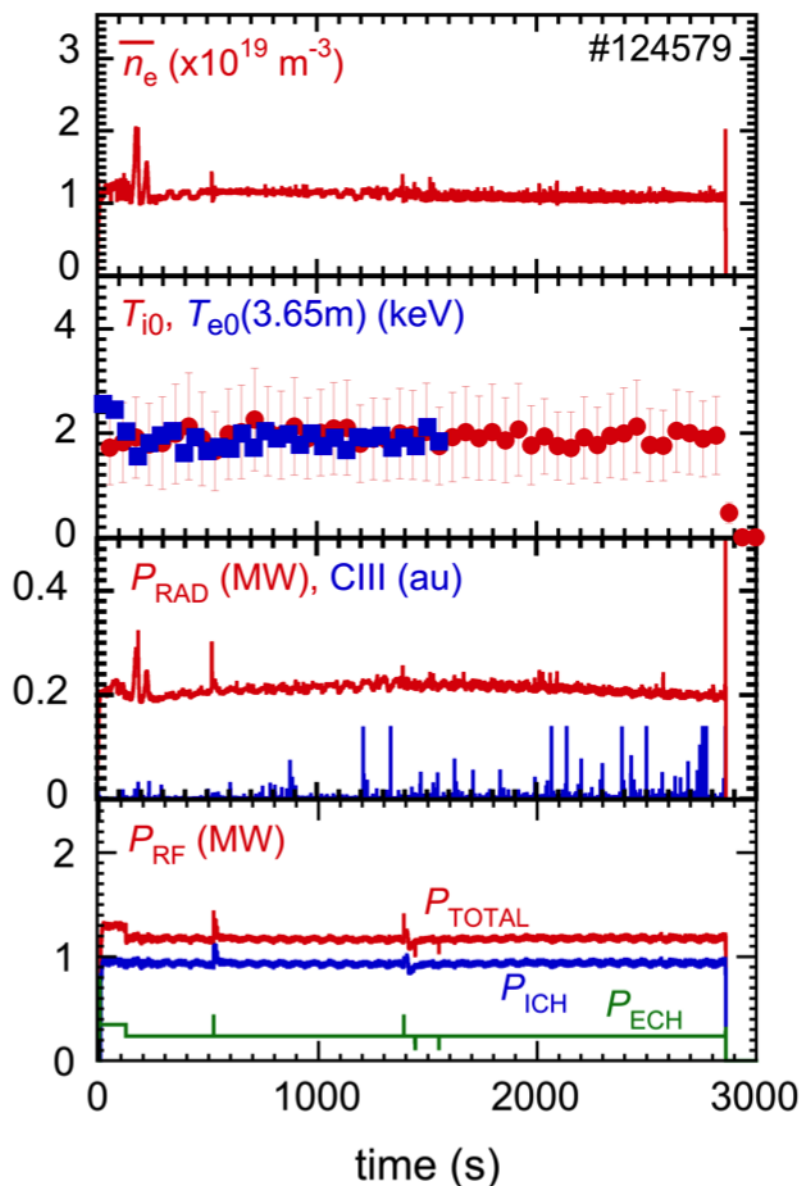
Thu. FIP/P5-3 T. Seki

- **Steady-state RF heating sources ~ 3.54 MW (ICH: 3MW, ECH: 0.54MW)**
Hydrogen minority heating (38.5MHz), Core electron heating (77GHz, 154GHz)
- **The integration of heating controls to decrease plasma degradations**
Scattering heating power, Maintaining heating power and plasma temperature
- **Adequate gas-fueling with the time evolution for PWI effect**
PID control method and supplies using several gas-fueling devices



- *The extension of steady-state plasma duration with MW-class heating, and the operation regions*
- *Result of ultra-long pulse plasma duration with $\tau_d \sim 48$ min, $P_{RF} \sim 1.2$ MW, $n_e \sim 1.2 \times 10^{19} \text{ m}^{-3}$, $T_e \sim T_i \sim 2$ keV, and $W_{inj} \sim 3.4$ GJ*
 - *Thermal behavior and typical temperatures*
Inhomogeneity of divertor heat flux
 - *The steady-state was terminated by sudden unintended entrance of the exfoliated mixed-material layers (MMLs) with continuous divertor erosion*
 - *Characteristics of the MMLs*
Thick region, the growth rate, the main elements, the physical property, and the trappable ability of He particles
 - *Preliminary estimation of He particle balance with the MMLs*
- *Summary and future plans*

Demonstration of ultra-long (~ 48 min) plasma discharge with MW-class plasma heating



Achievement parameters:

$n_e \sim 1.2 \times 10^{19} \text{ m}^{-3}$, $T_i \sim T_e \sim 2 \text{ keV}$, $\tau_d \sim 2859 \text{ sec}$,
 $P_{\text{RF}} \sim 1.2 \text{ MW}$ ($P_{\text{ICH}} \sim 0.94 \text{ MW}$, $P_{\text{ECH}} \sim 0.26 \text{ MW}$),
 $W_{\text{heat}} \sim 3.4 \text{ GJ}$, $n_{i0} \tau_E^* T_{i0} \sim 3.5 \times 10^{18} \text{ keV m}^{-3} \text{ s}$

Development of steady-state heating and PWI devices were effectively carried out

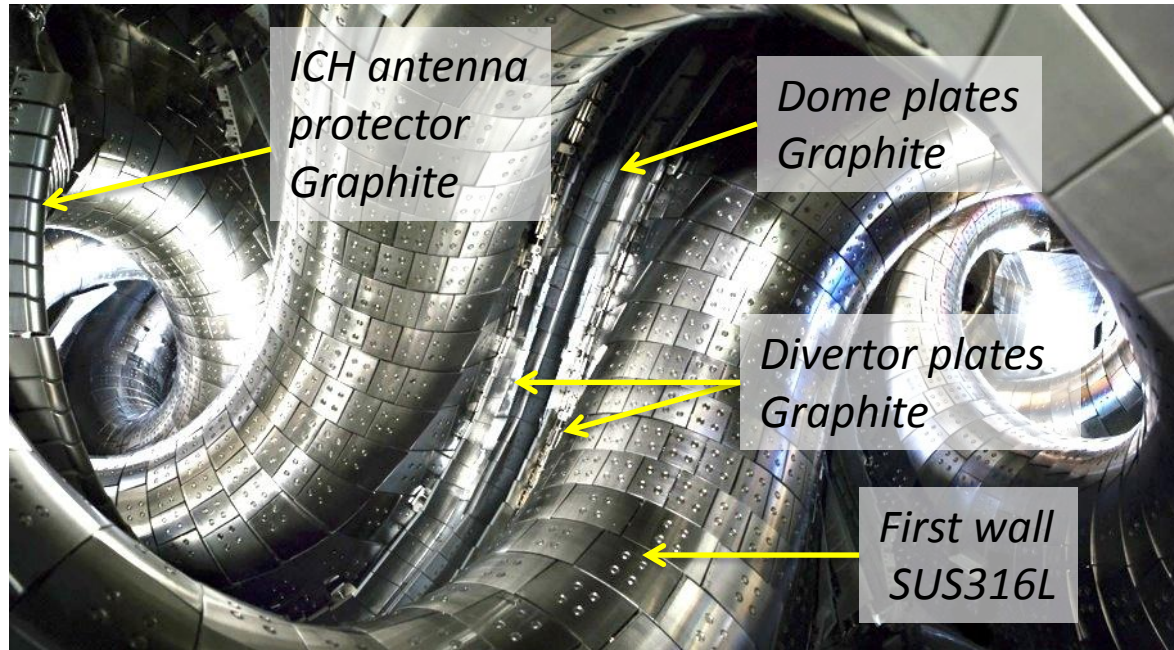
- *Controlling electron density with PWI effect*
- *Steady-state temperature $T_e \sim T_i$*
- *Spark mitigation and no impurity accumulation*
- *Stable RF heating with event triggering heating power boost*
- *The integration of heating power systems*

These improvements produced a robust plasma discharge.

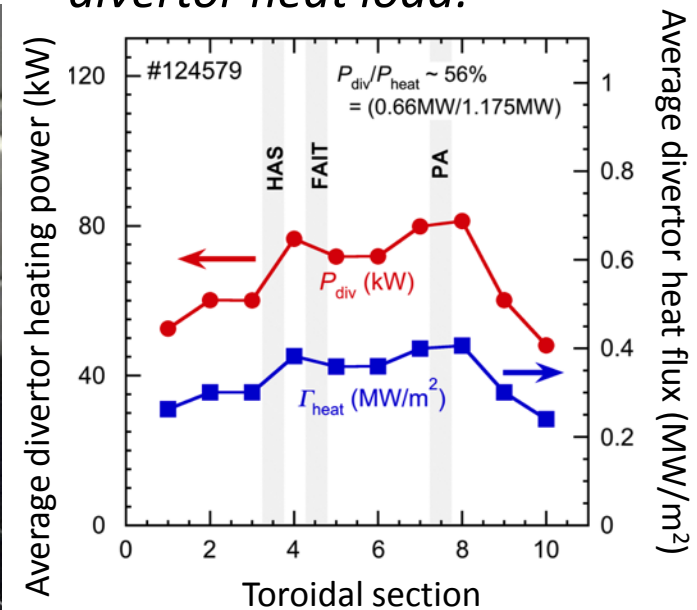
Thermal behavior, toroidal uniformity of divertor heat load, and total heat balance



$P_{RF} \sim 1.2\text{MW}$, $n_e \sim 1.2 \times 10^{19} \text{ m}^{-3}$, $T_e \sim T_i \sim 2 \text{ keV}$, 48 min.



Toroidal ununiformity of divertor heat load:



Total power balance:

Radiation P_{rad} : 17 %

Divertor P_{div} : 56 %

Other P_{other} : 27 %

Average heat flux

Γ_{heat} : 0.33 MW/m²

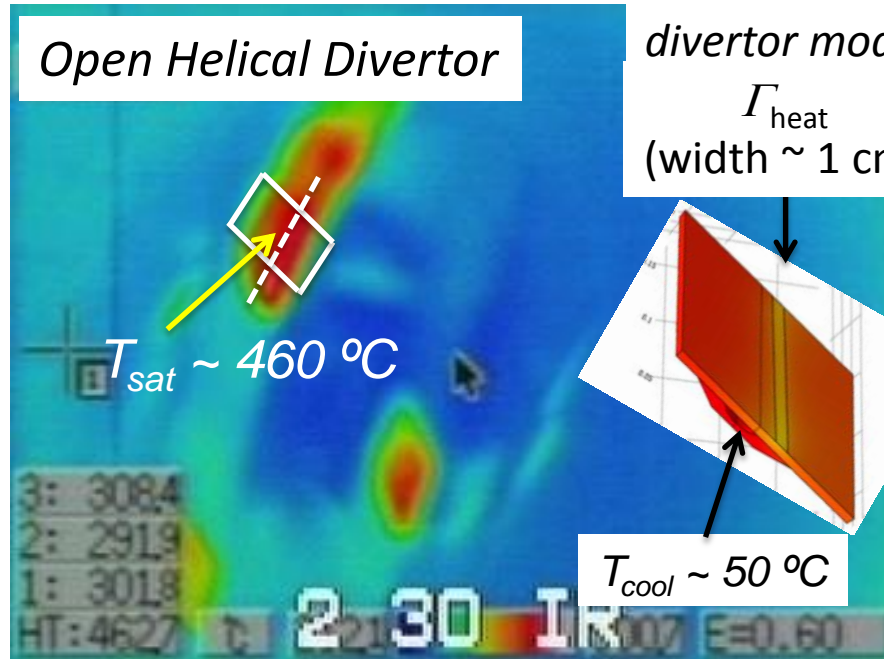
(0.25 ~ 0.4 MW/m²)

| Name | Protector surface (IR) | Divertor surface (IR) | Divertor (thermocouple) | First wall (thermocouple) |
|-----------------------|------------------------|-----------------------|-------------------------|---------------------------|
| Temp. (°C) | 300-900 | 460 | 180-270 | 40 -110 |
| Saturation time-scale | ~ 800 s | ~ 600 s | ~ 700 s | > 3000 s |
| Material | Graphite | Graphite | Graphite | SUS316L |

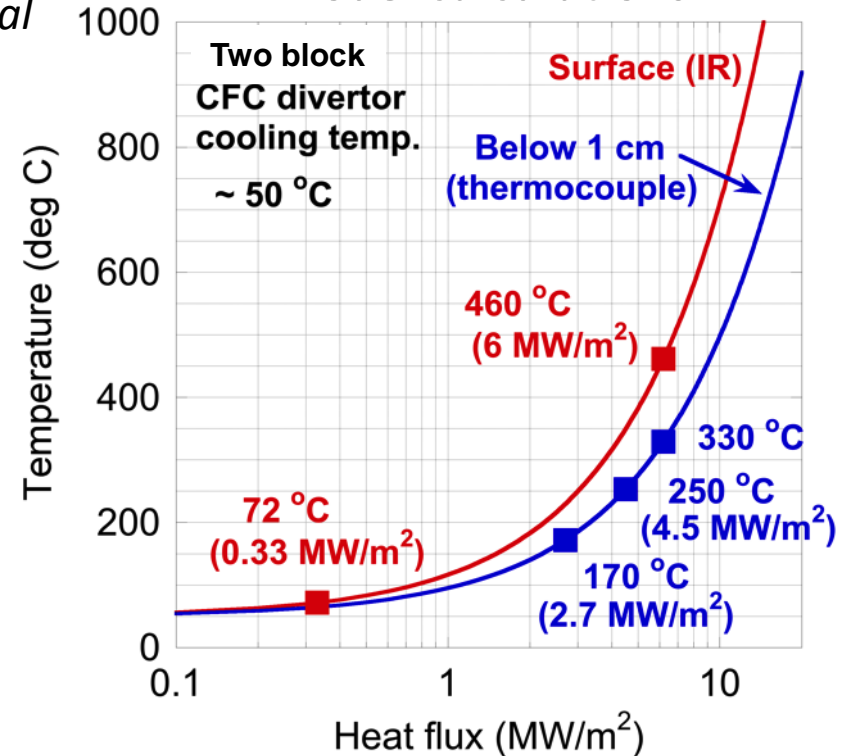
Evaluation of the local heat flux on the particular divertor plates (Poloidal uniformity of divertor heat flux)



A photo of Infra-red camera



Model calculations

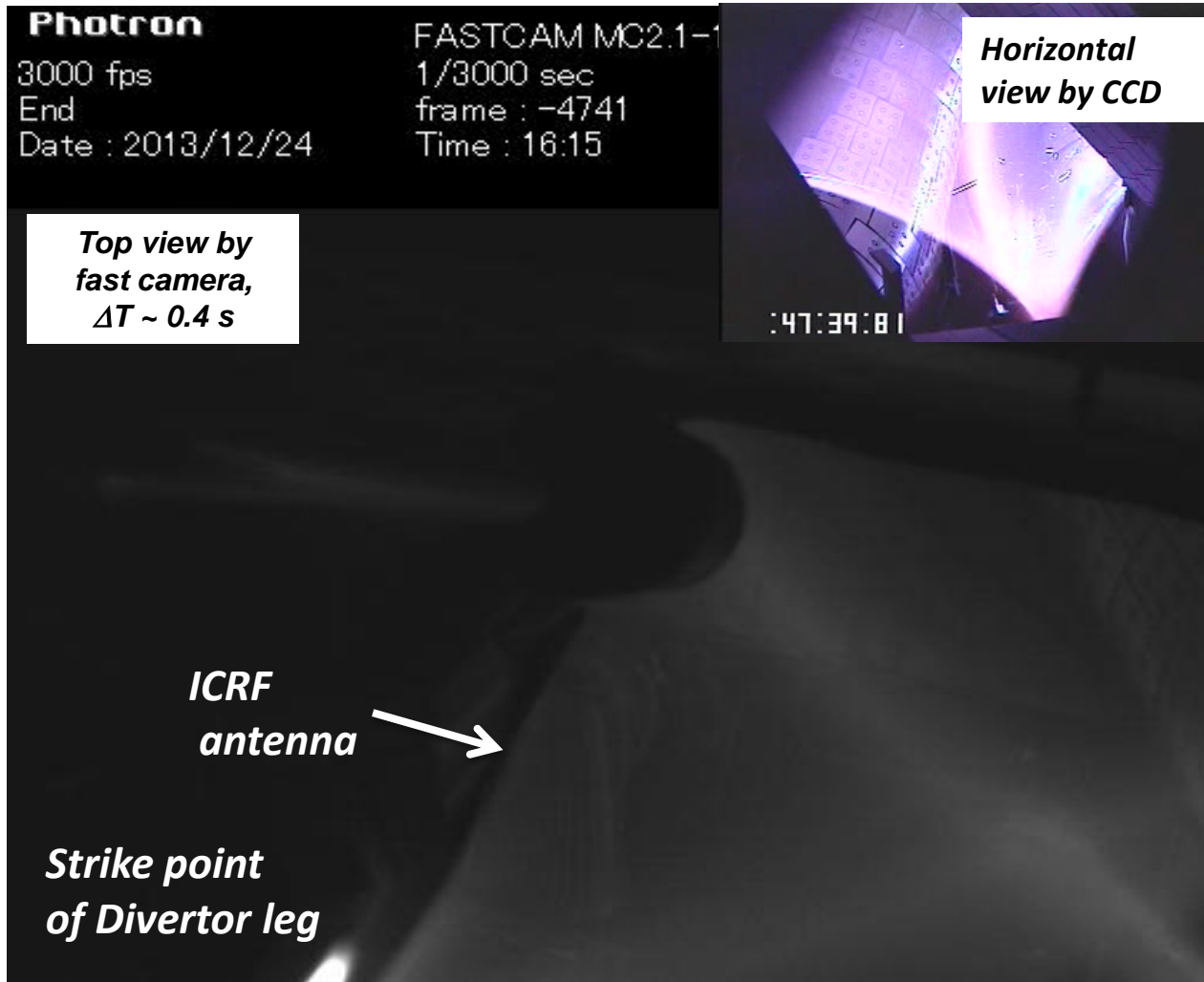
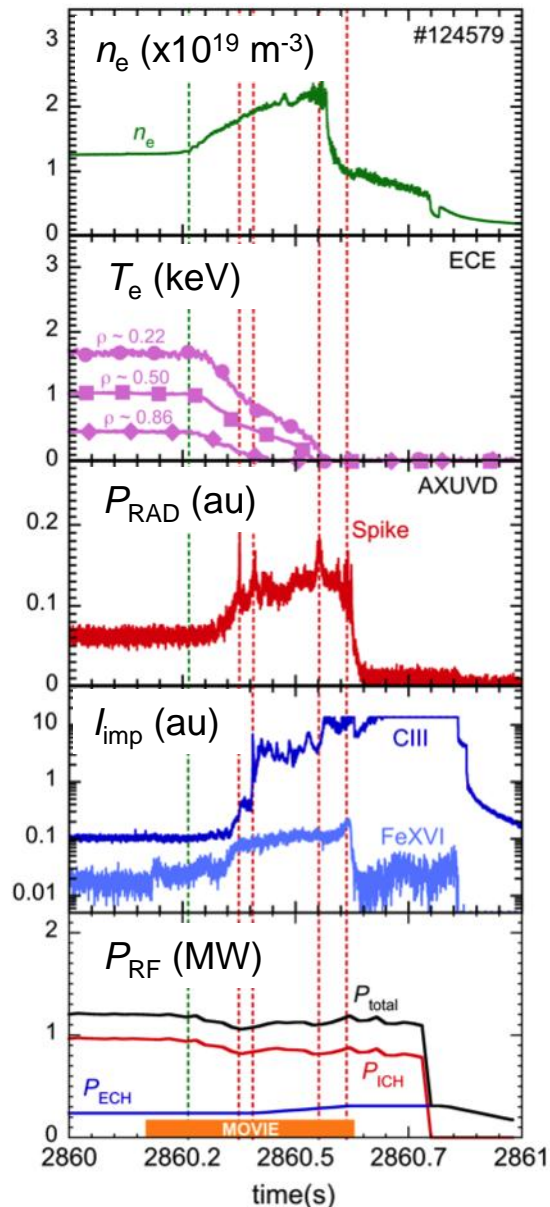


- Large discrepancy between experiment result ($460 \text{ } ^\circ\text{C}$) and the calculation ($T_{sat} \sim 72 \text{ } ^\circ\text{C}$) with average heat flux ($\Gamma \sim 0.33 \text{ MW/m}^2$)
- The peak factor of poloidal inhomogeneity of divertor heat flux was ~ 18 (open helical divertor) and ~ 14 (closed helical divertor)
- The heat flux of particular carbon divertor plates ($\sim 6 \text{ MW/m}^2$) in $P_{RF} \sim 1.2 \text{ MW}$ and $\tau_d \sim 48 \text{ min}$ come close ITER relevant heat flux ($\sim 5\text{-}10 \text{ MW/m}^2$)



- *The extension of steady-state plasma duration with MW-class heating, and the operation regions*
- *Result of ultra-long pulse plasma duration with $\tau_d \sim 48$ min, $P_{RF} \sim 1.2$ MW, $n_e \sim 1.2 \times 10^{19} \text{ m}^{-3}$, $T_e \sim T_i \sim 2$ keV, and $W_{inj} \sim 3.4$ GJ*
 - *Thermal behavior and typical temperatures*
Inhomogeneity of divertor heat flux
 - *The steady-state was terminated by sudden unintended entrance of the exfoliated mixed-material layers (MMLs) with continuous divertor erosion*
 - *Characteristics of the MMLs*
Thick region, the growth rate, the main elements, the physical property, and the trappable ability of He particles
 - *Preliminary estimation of He particle balance with the MMLs*
- *Summary and future plans*

Plasma collapse with strong and continuous impurity entrances (Steady-state was terminated by exfoliating the deposition layers.)



Collapsed by widely and continuously exfoliating the deposition layer caused by continuous divertor erosion

divertor

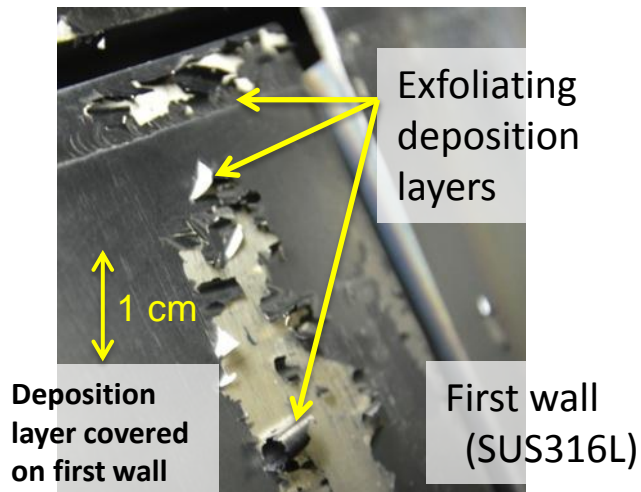


- *The extension of steady-state plasma duration with MW-class heating, and the operation regions*
- *Result of ultra-long pulse plasma duration with $\tau_d \sim 48$ min, $P_{RF} \sim 1.2$ MW, $n_e \sim 1.2 \times 10^{19} \text{ m}^{-3}$, $T_e \sim T_i \sim 2$ keV, and $W_{inj} \sim 3.4$ GJ*
 - *Thermal behavior and typical temperatures*
Inhomogeneity of divertor heat flux
 - *The steady-state was terminated by sudden unintended entrance of the exfoliated mixed-material layers (MMLs) with continuous divertor erosion*
 - *Characteristics of the MMLs*
Thick region, the growth rate, the main elements, the physical property, and the trappable ability of He particles
 - *Preliminary estimation of He particle balance with the MMLs*
- *Summary and future plans*

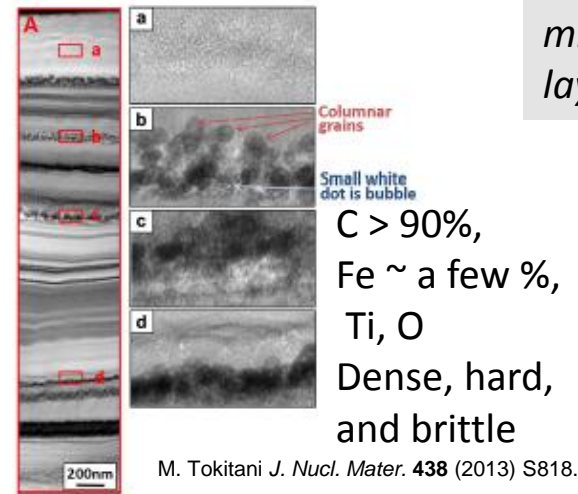
Characteristics of carbon-rich mixed-material layers (MMLs) and the exfoliation size at the plasma collapse



Exfoliating small flakes from the first wall



The accumulation of a mixed-material layer and its elements



Exfoliated the carbon-rich mixed-material layer

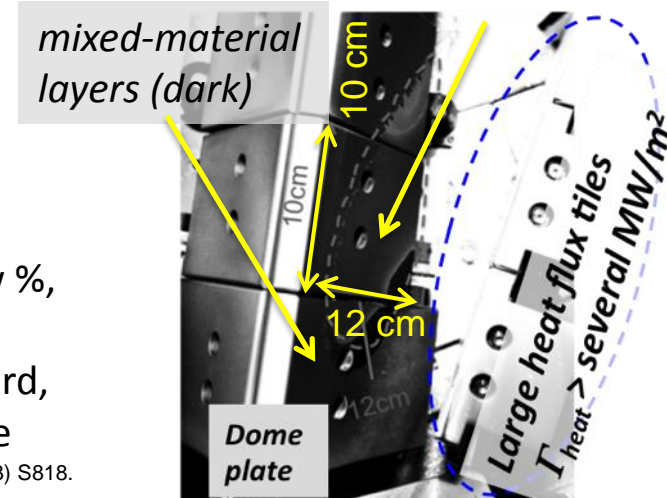


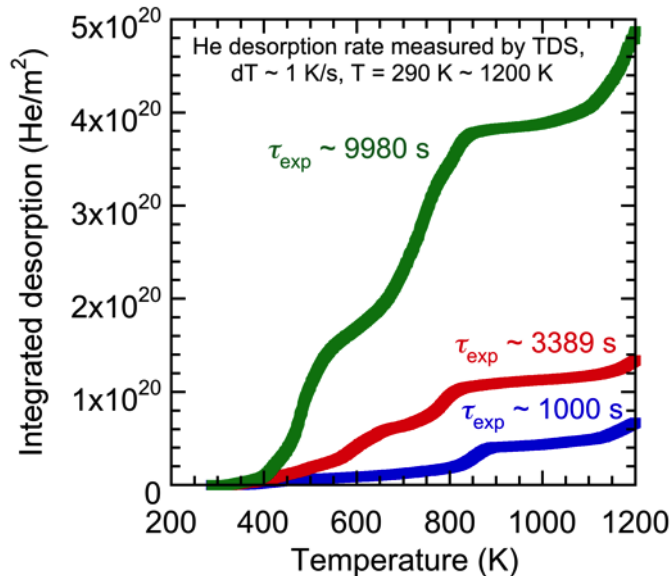
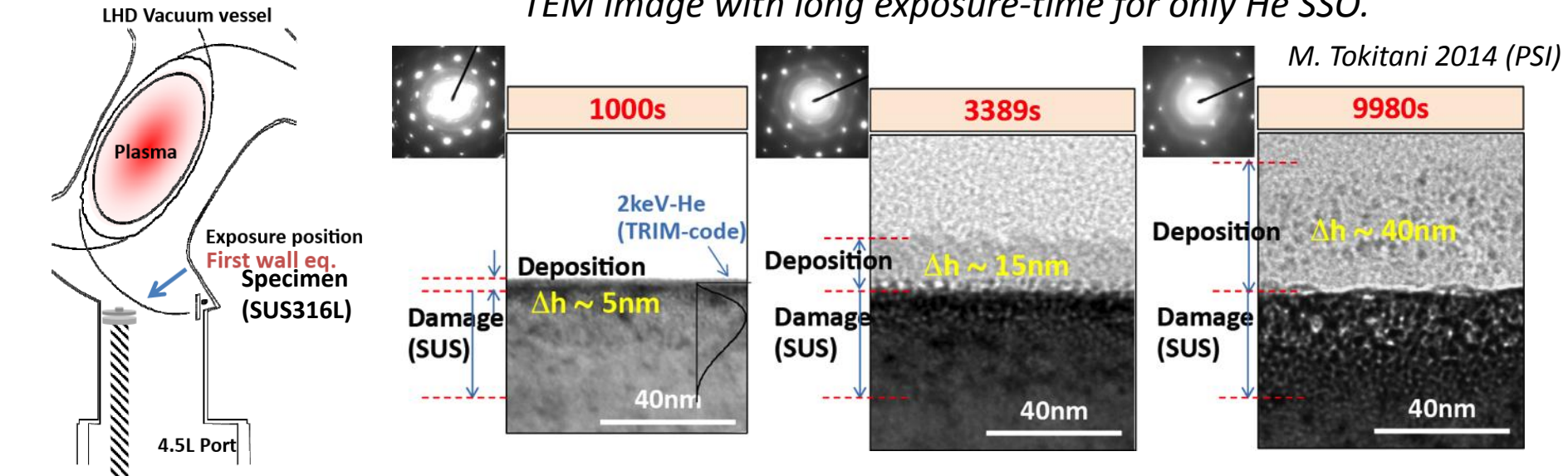
Fig. 3. Right series (a-d): High resolution TEM micrographs corresponding to the small frames in (A).

- MMLs: carbon (>90%) and iron (~ a few %), dense, hard, and brittle
- Plasma collapse occurred due to continuous exfoliation (~ 10 cm x 12 cm), and this will be a critical issue to maintain steady-state plasma.
- The thick MML was observed around the particular carbon divertor plates with the large heat flux and the geometrical dense region.

Growth rate of carbon-rich mixed-material layers and the trappable particles by the fresh layer at the first wall position



TEM image with long exposure-time for only He SSO.



| Exposure time (s) | 1000 | 3389 | 9980 |
|--|------|------|------------------|
| Thickness (nm) | 5 | 15 | 40 |
| C ($\times 10^{19}$ atoms/ m^2) | | 260 | 370 (98%) |
| Fe ($\times 10^{19}$ atoms/ m^2) | | 3.0 | 3.8 (1-2%) |
| Mo ($\times 10^{19}$ atoms/ m^2) | | 0.07 | 0.23 |
| Desorption ($\times 10^{19}$ He/ m^2) | 0.63 | 1.88 | 10.6 (300-600 K) |

Predicted He particle retention rate:

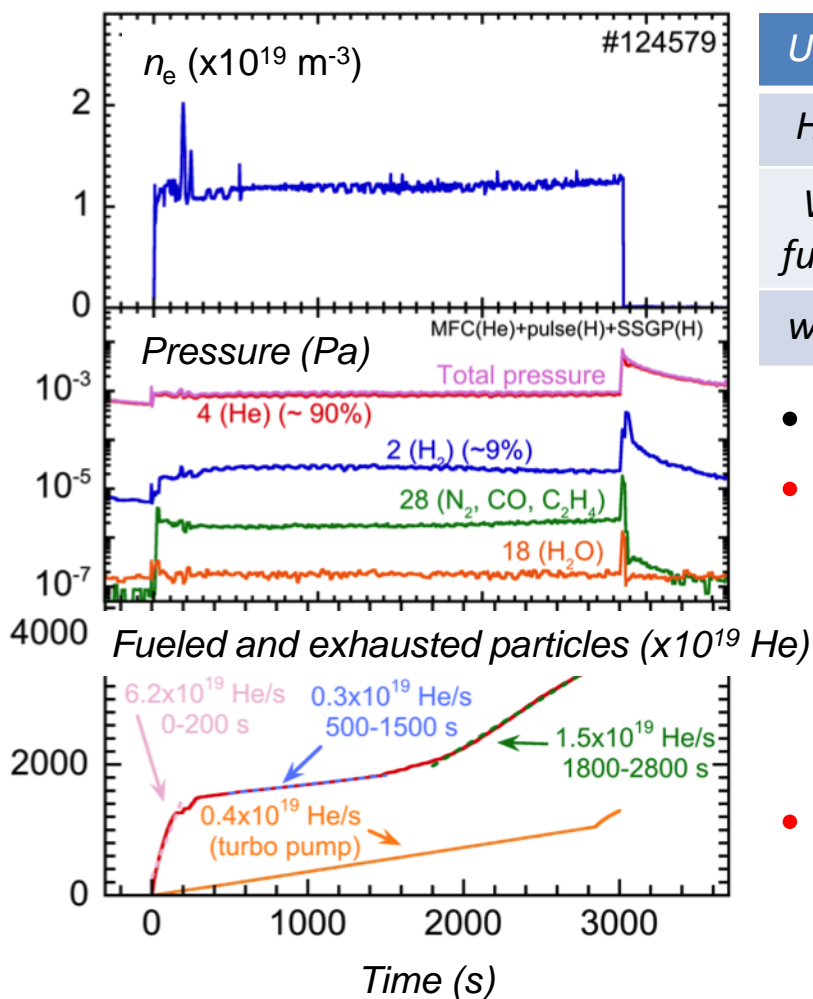
$\sim 1.6 \times 10^{16} \text{ He}/(\text{m}^2 \text{ s}) (= 2.34 \times 10^{18} \text{ He/s (20\%/730 m}^2))$

Fresh mixed-material layers (MMLs) affecting wall-pumping rate for He particles in several ten minutes



Three fueling phases
 6.2 (0-200s), 0.3 (500-1500s),
 1.5 (1800-2800s) ($\times 10^{19}$ He/s).

He particle balances w/wo the effect of the MMLs
Wall-pumping: absorption (>0), desorption (<0)
 (Assumption: MMLs covered 26% of the PFCs.)



| Unit: $\times 10^{19}$ He/s | 0-200 s | 500-1500 s | 1800-2800 s |
|----------------------------------|---------|-----------------------|----------------------|
| He fueling rate | 6.22 | 0.28 | 1.48 |
| Wall-pumping fuel – pump(0.4) | 5.85 | -0.09 (Desorption) | 1.11 (Absorption) |
| w/ MMLs (26%) | 5.48 | -0.46 | 0.74 |

- Neutral pressure for He ~ constant
- Particle fueling-rate recovered after several ten minutes ($\sim 48 \text{ m}^3/\text{s}$)
 The recovered wall-pumping rate was large. $1.11 \times 10^{19} \text{ He/s} \sim 95\% > 0.37 \times 10^{19} \text{ He/s}$ with 26% (realistic covered area)
- The study of the actual thickness map of MMLs will be more important for assessing accurate global particle balance.

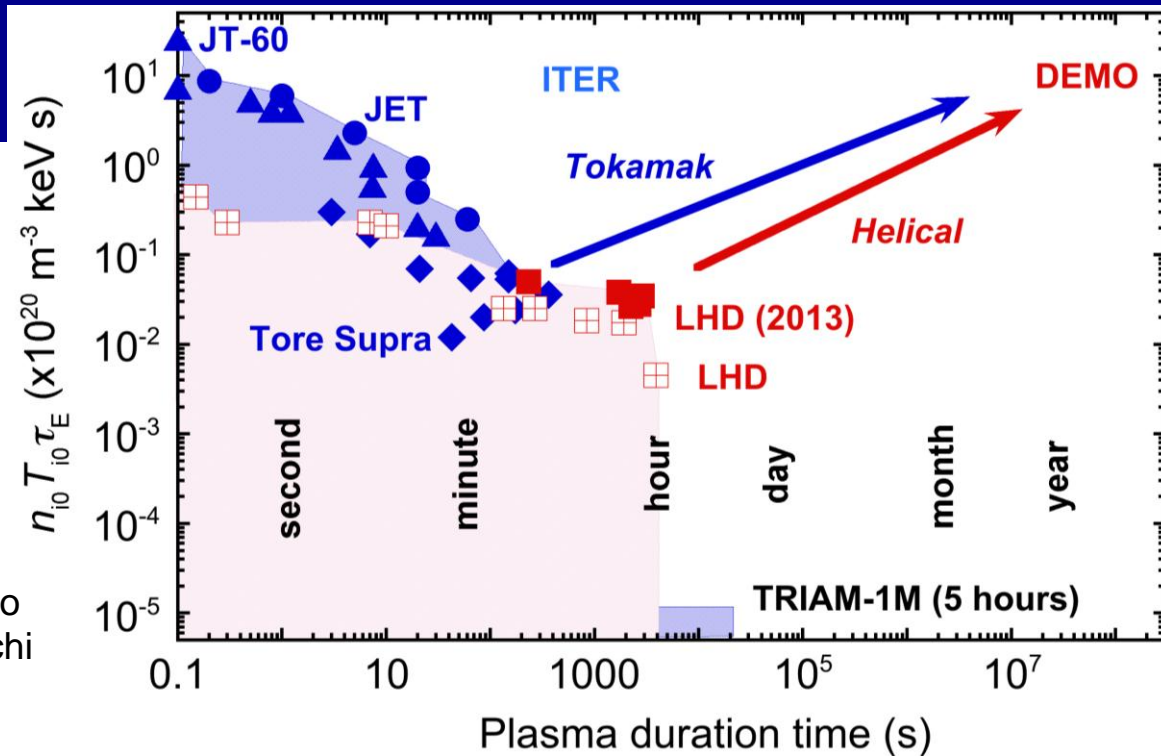
Extending steady-state plasma performance with MW-class plasma heating for He plasma

- *Well controlled ICH, core electron heating (77 GHz, 154 GHz), event triggering boost of RF power power, and adequate gas fueling made robust plasmas with e-ITB profile.*
- *Ultra long-pulse ($\tau_d \sim 48$ min, $P_{RF} \sim 1.2$ MW, $W_{inj} \sim 3.4$ GJ):
 $n_e \sim 1.2 \times 10^{19} \text{ m}^{-3}$, $T_{e0} \sim T_{i0} \sim 2$ keV, $n_{i0} T_{i0} \tau_E \sim 3.5 \times 10^{18} \text{ m}^{-3} \text{ keV s}$*
- *Long-pulse ($\tau_d \sim 6$ min, $P_{RF} \sim 2.3$ MW, first trial)
 $n_{e, max} \sim 3.3 \times 10^{19} \text{ m}^{-3}$, $T_{e0} \sim T_{i0} \sim 1.5$ keV*

The surface condition of PFCs was affected by continuous divertor erosion and ion impacts to the surfaces over several ten minutes.

- *Carbon-rich mixed-material layers (MMLs) were grown around particular carbon divertor plates (geometrical dense and continuous large heat flux)*
- *Growth rate ~ 15 nm/hour*
- *The physical property \sim hard, dense, brittle, C ($> 98\%$), Fe (\sim a few %)*
- *Retention rate of He particles $\sim 1.6 \times 10^{16}$ He/m² s (first wall position)*

Future plans



For high-performance SSO,

- Performing the improvement of heating quality and the optimization
- **Maintaining plasma performance in weak wall-pumping with ion impacts**

For mixed-material layers (MMLs)

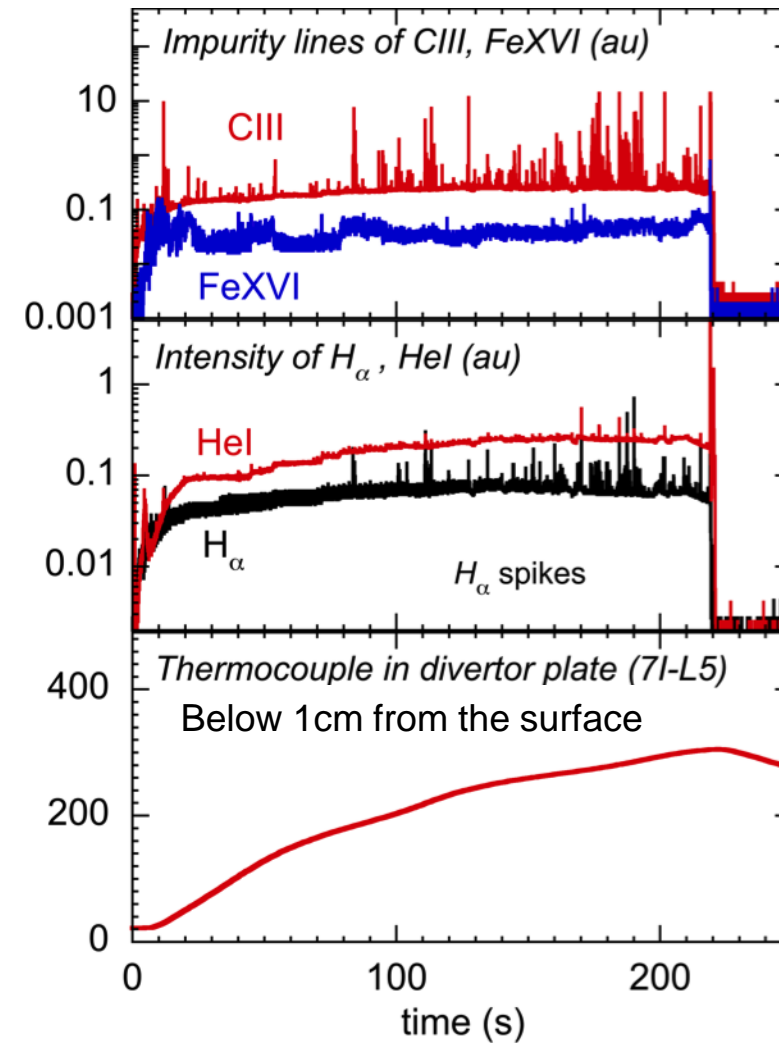
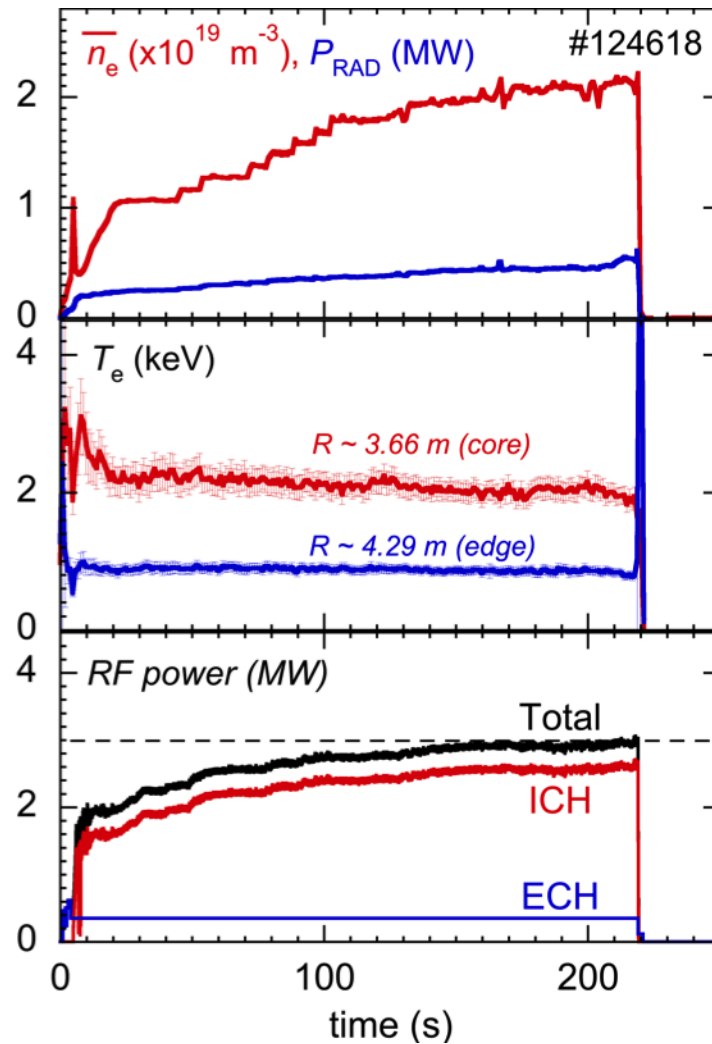
- Accurate assessments of the MMLs in various plasma parameters
- **Revealing the growth and exfoliating mechanism of the MMLs**
- Investigating the other MMLs (ex. W) caused by unavoidable divertor erosion

References

First trial of the higher-power long-pulse plasma discharge (2-3MW, > 200 sec)



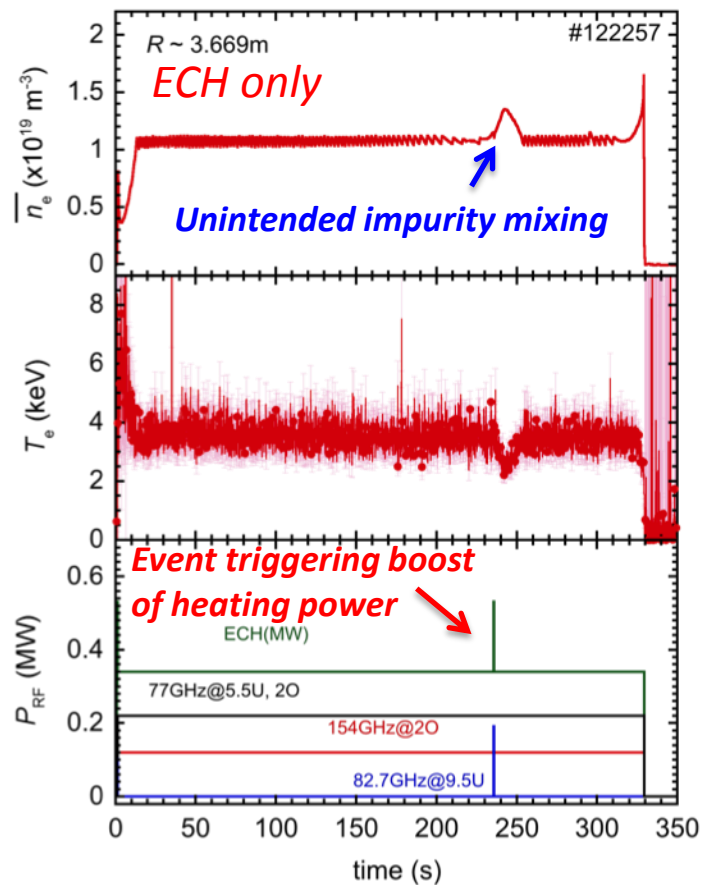
Command values of RF heating power and electron density were manually increased after confirming the health of heating and PWI devices.



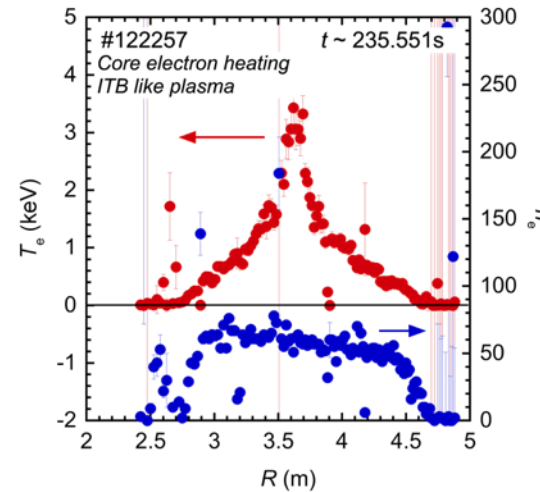
Core electron heating and event triggering boost of heating power make a robust steady-state plasma



Core electron heating power was increased (77GHz and 154GHz), $P_{ECH} \sim 0.34\text{MW}$.

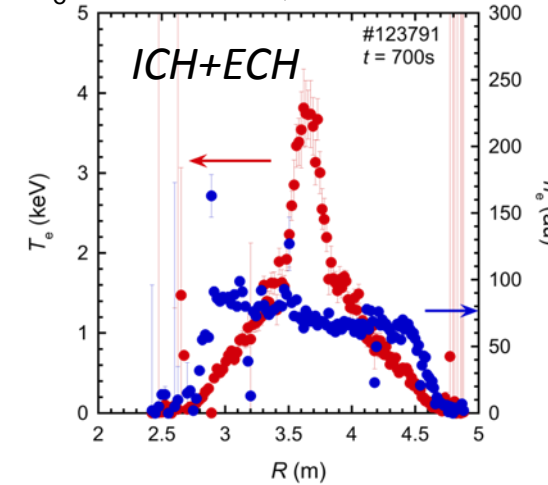


e-ITB plasma was sustained during SSO



e-ITB plasma also was sustained using ECH+ICH.

$P_{ICH+ECH} = 0.93\text{MW}$ ($P_{ECH}=0.33\text{MW}$)
 $n_e \sim 1 \times 10^{19} \text{ m}^{-3}$, 11 min.

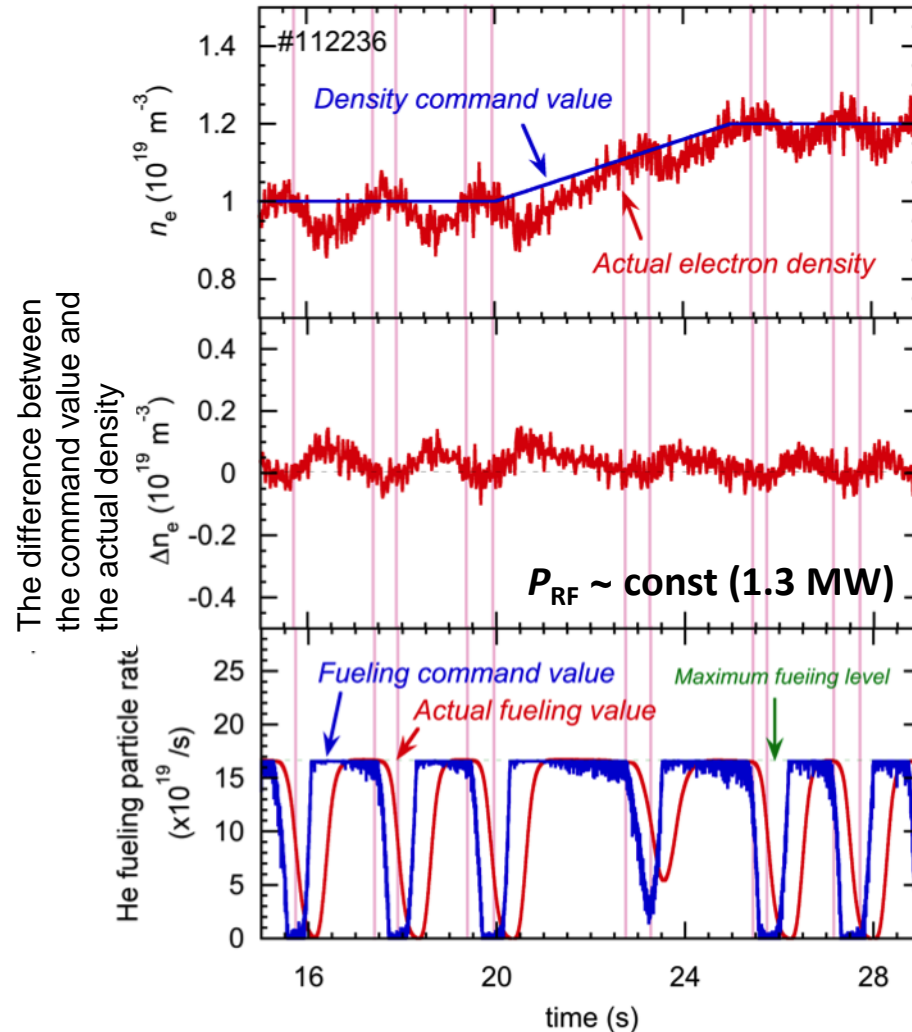


- Increasing the power ($>0.3\text{MW}$) of core electron heating (77, 154GHz) easily made e-ITB plasma during SSO, and it kept core electron temperature stable and high.
- Event triggering boost of heating power effectively carried out to maintain the plasma.

The particle fueling using the proportional-integral-derivative (PID) method was effectively carried out with the time evolution of wall-pumping rate.

First trial of density control using the PI/PID method and plasma density followed the preprogrammed command value.

In order to adopt various wall-pumping conditions, the integral method is required.



$$\Delta n_e(t) = n_{target}(t) - n_{fir}(t) \quad : \text{Differential part}$$

$$V_{fuel}(t + dt) = \alpha_1 \Delta n_e(t + dt) + b_1(t + dt) \quad : \text{fast}$$

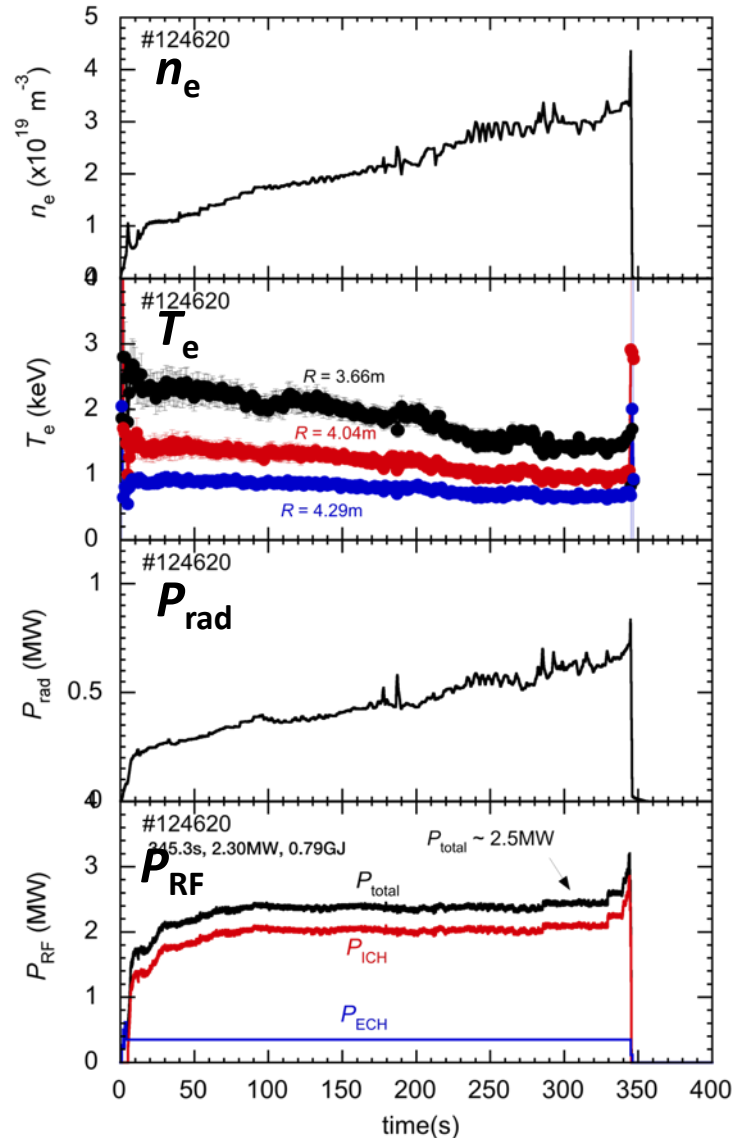
$$b_1(t + dt) = V_{fuel}(t) + \frac{1}{dt} \int_t^{t+dt} \beta_1 \Delta n_e(t) dt \quad : \text{slow}$$

Electron density followed the command value using the PID method.

Adequate gas-fueling was achieved with time delay for gas-fueling during long-pulse discharges.

This gas-fueling rate depends on the unintended impurity mixing events, too.

Confirming the stable sustainable density with the RF heating power of 2-3 MW.



Relatively high density operation
 $n_e^{max} \sim 3.3 \times 10^{19} \text{ m}^{-3}$, $T_e \sim 1.5 \text{ keV}$,
 $P_{RF} \sim 2.3 \text{ MW}$, $\tau_d \sim 345 \text{ sec}$

In order to confirm the stable sustainable density with $P_{RF} \sim 2-3 \text{ MW}$, the target value for density was gradually increased.

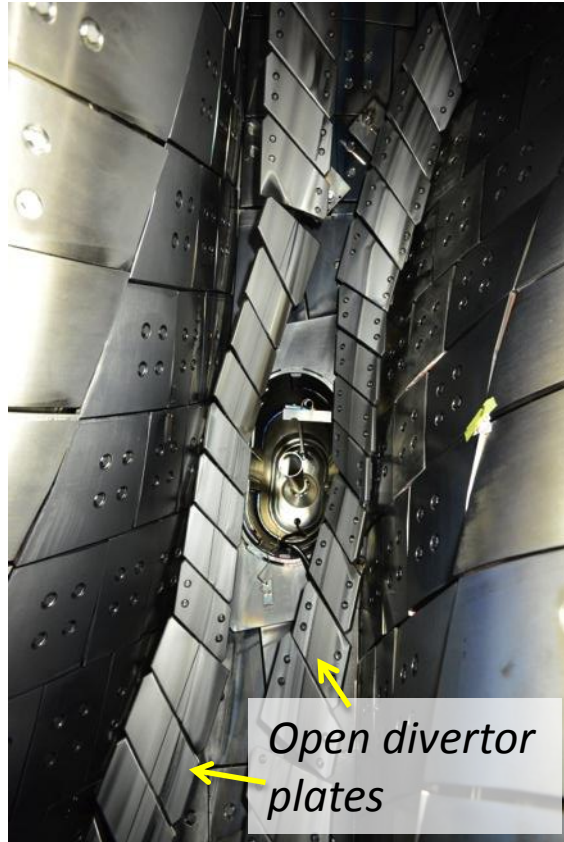
When the density reached $3 \times 10^{19} \text{ m}^{-3}$, the ratio of the total radiation power for ejection power reached 28 %. (Usual operation is $\sim 17\%$)

Heating quality was degraded, and it is necessary to confirm the minority ratio on the cyclotron resonance.

LHD and the divertor configurations



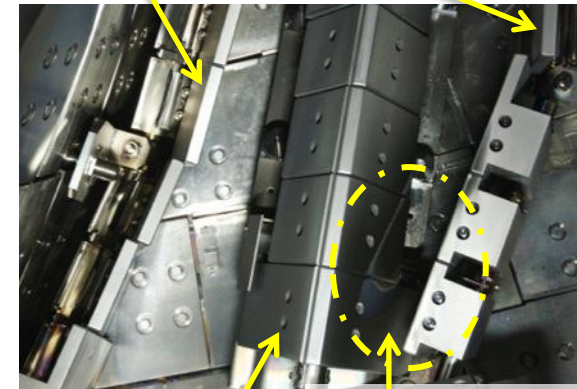
Open helical divertor (OHD)



Closed helical divertor (CHD)



Standing divertor plates



Dome plates Geometrically dense

Divertor configuration

OHD: 3

CHD: 1-2, 4-10

Footprint $S \sim 2 \text{ m}^2$

(100m x 2 lines) x 1 cm

Typical device parameters:

Volume:

Inside vessel $\sim 210 \text{ m}^3$

Plasma $\sim 30 \text{ m}^3$ ($R_{ax} \sim 3.9\text{m}$, $a \sim 0.6\text{m}$)

Surface:

PFCs $\sim 780 \text{ m}^2$

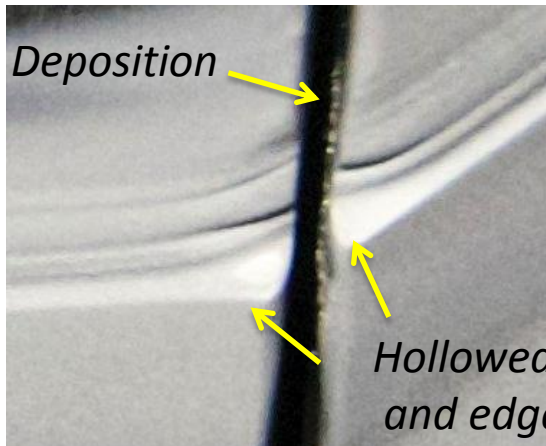
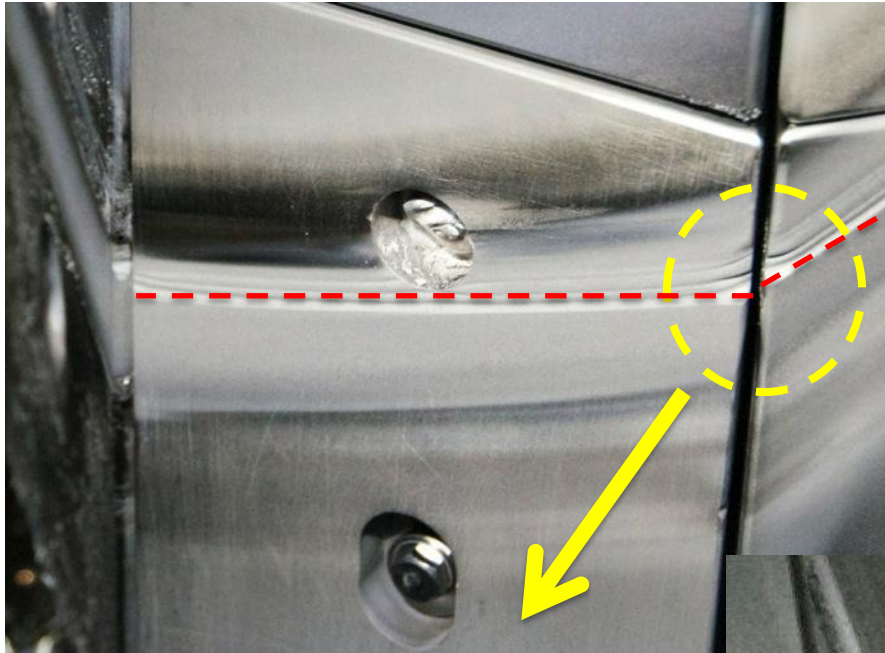
First wall $\sim 730 \text{ m}^2$ (SUS316L)

Divertor plate $\sim 50 \text{ m}^2$ (Graphite)

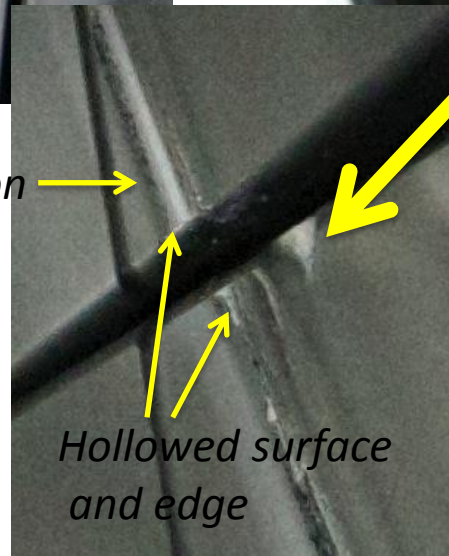
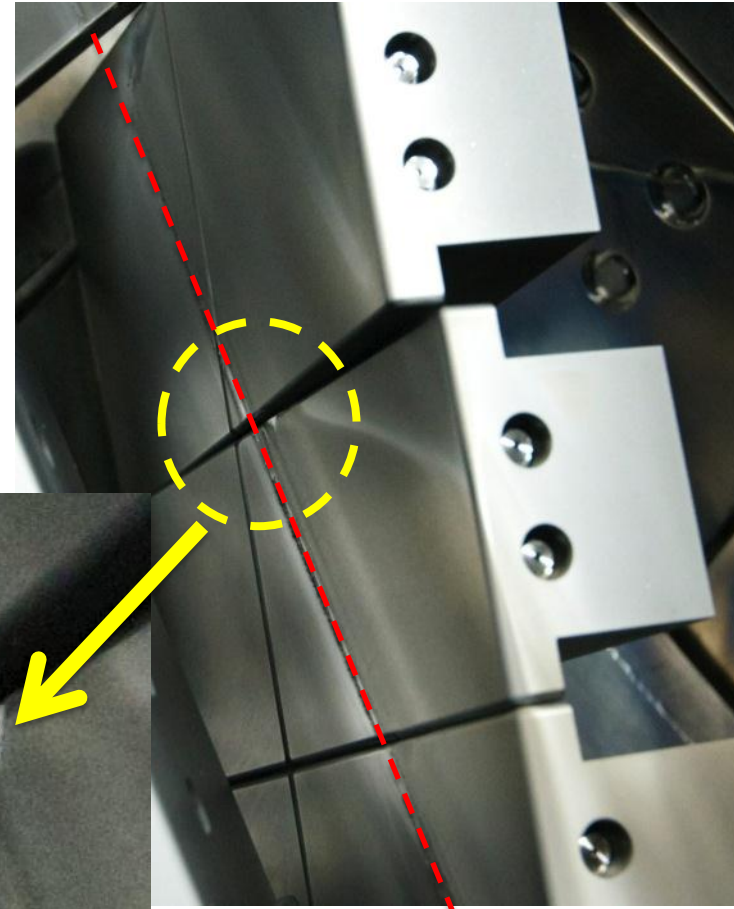
Progressing continuous erosion with no degradation of divertor heat removal



Isotropic carbon plate (IG-43)



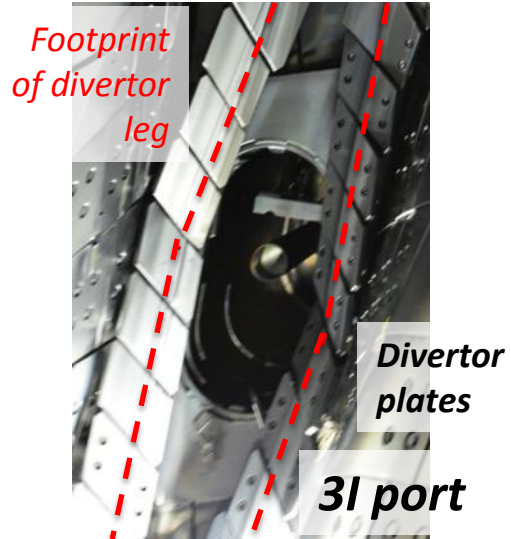
CFC plate (CX-2002)
Carbon-fiber-composite



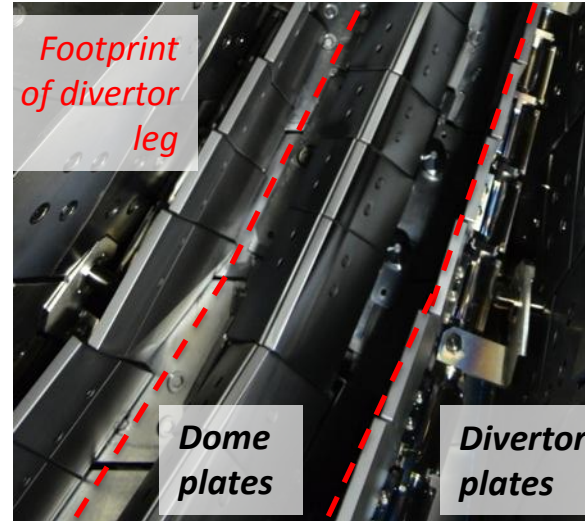
Carbon-rich MMLs grew around particular divertor plates with relatively large heart flux and at the geometrical dense region.



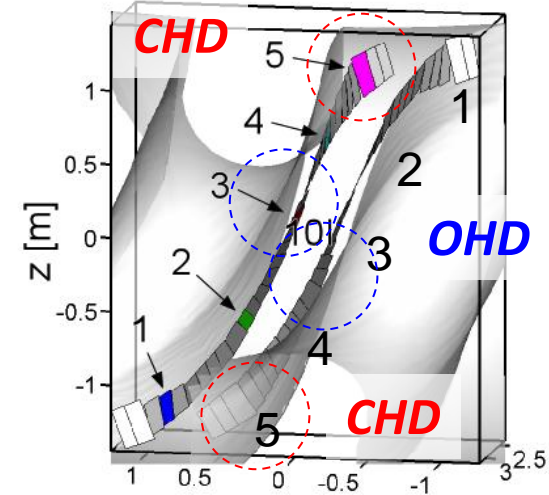
Open-helical divertor (OHD)



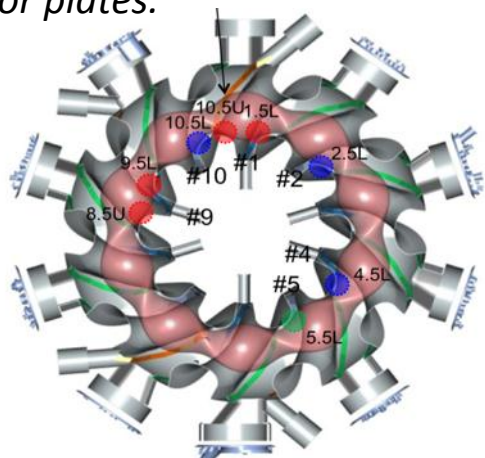
Closed-helical divertor (CHD)



Schematic view of large heat flux divertor



Thick mixed-material layer was observed around particular divertor plates.



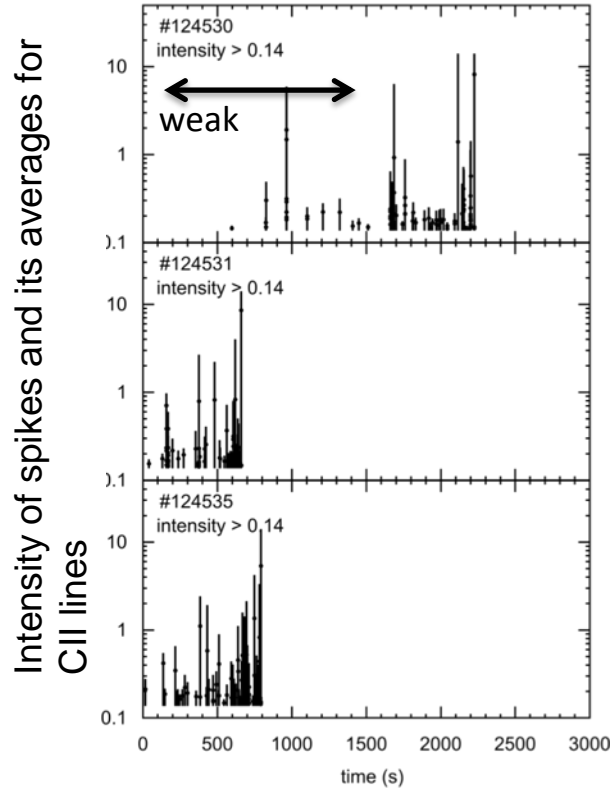
- There is large uniformity of divertor heat flux profile in poloidal direction.
- **Mixed-material layer with continuous large heat flux easily grew on the geometrical dense region (CHD) rather than on the open region (OHD).**
- How about is the duration time for the thickness of MML and the effect of particle balances ?

Carbon impurity was extended on the hot divertor, and it seems to depend on the deposition layer



After repeated high power (~30MW) short pulse discharges

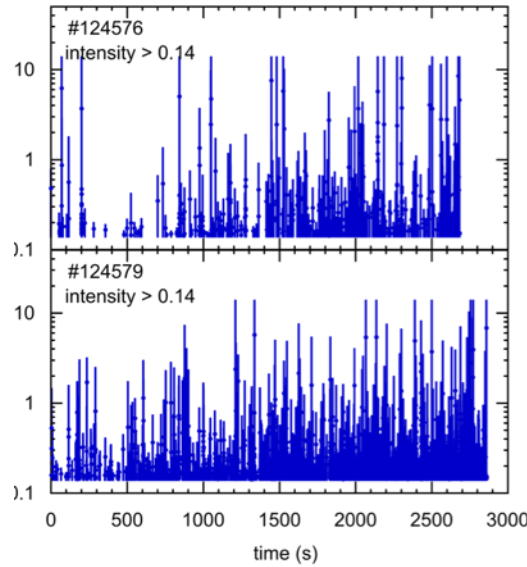
1st day (12/20, Fri)



After long pulse discharge with $n_e \sim 10^{19} \text{ m}^{-3}$, 2 keV, and 1MW, spikes of carbon impurity were clearly increased.

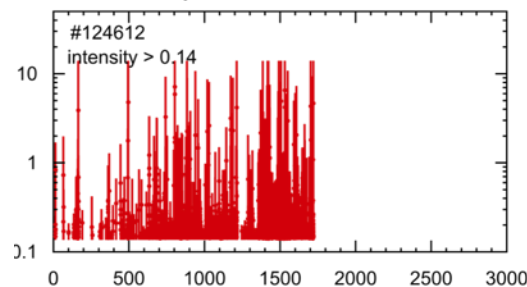
After baking, Ti gettering and refreshed cryo-pump

2nd day (12/24, Tue)

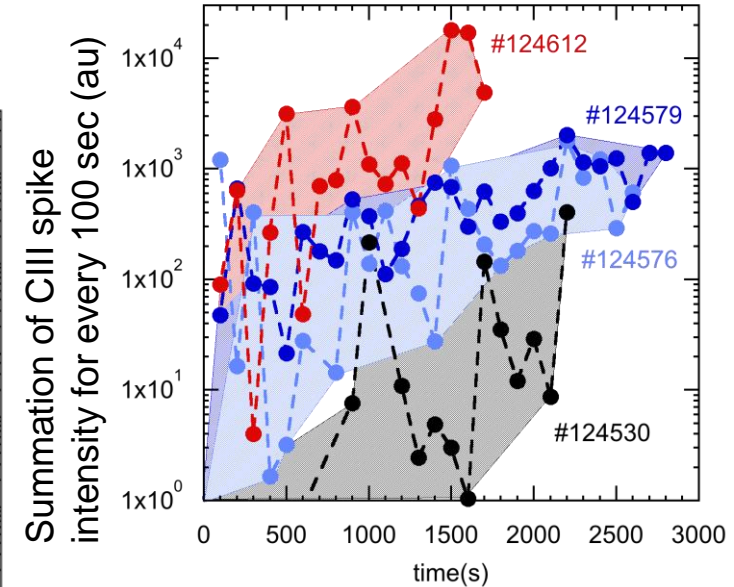


Only main pumping

3rd day (12/25, Wed)



Time evolution and history of carbon spikes



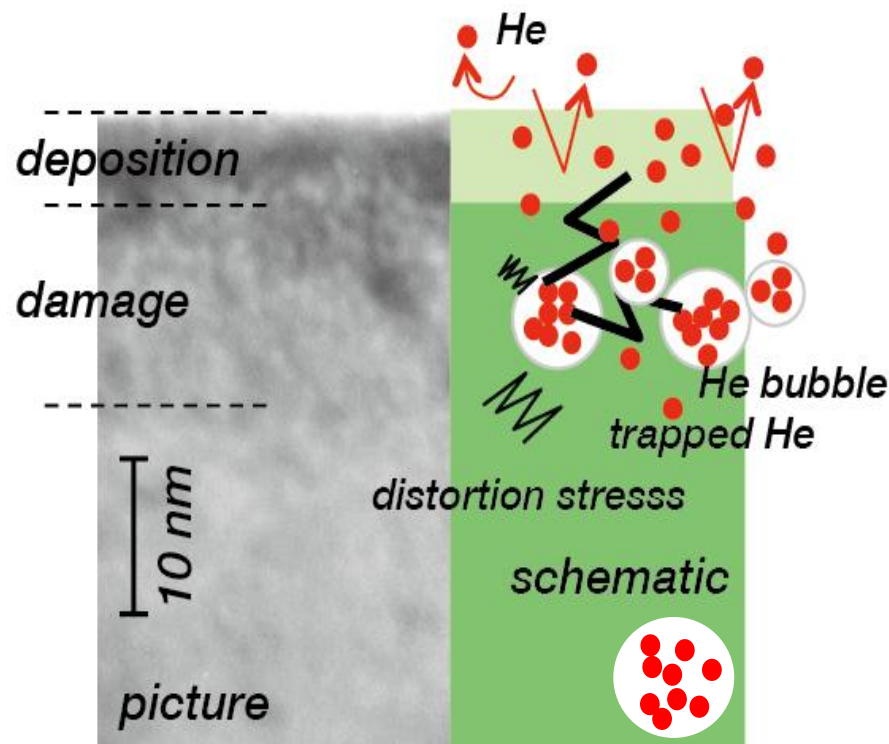
Intensity and frequency of carbon spikes were increased as plasma discharge was extended with the divertor temperature $\sim 500 \text{ }^\circ\text{C}$ (hot divertor).

The spikes were strongly related to the thickness of deposition layer and the history of plasma durations.

Exfoliation model of the mixed-material layers (MMLs)



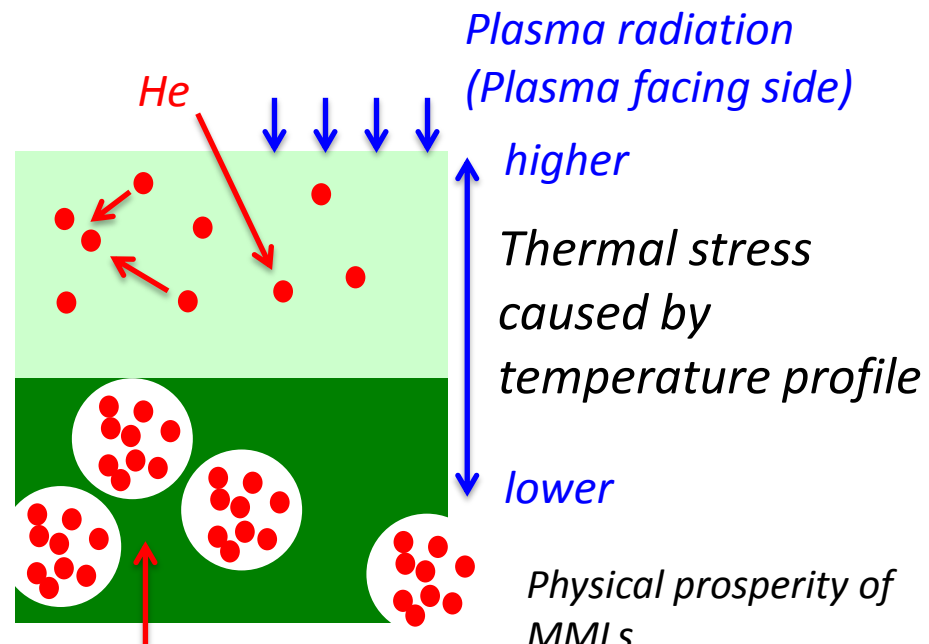
Stainless steel specimen was only exposed by He long-pulse plasma duration with exposure time ~ 1000 sec.



Picture of the exfoliating MMLs from the first wall

Two exfoliation models of the mixed-material layers

- Thermal stress with the temperature profile
- Explosive release by the cohesion of He bubbles



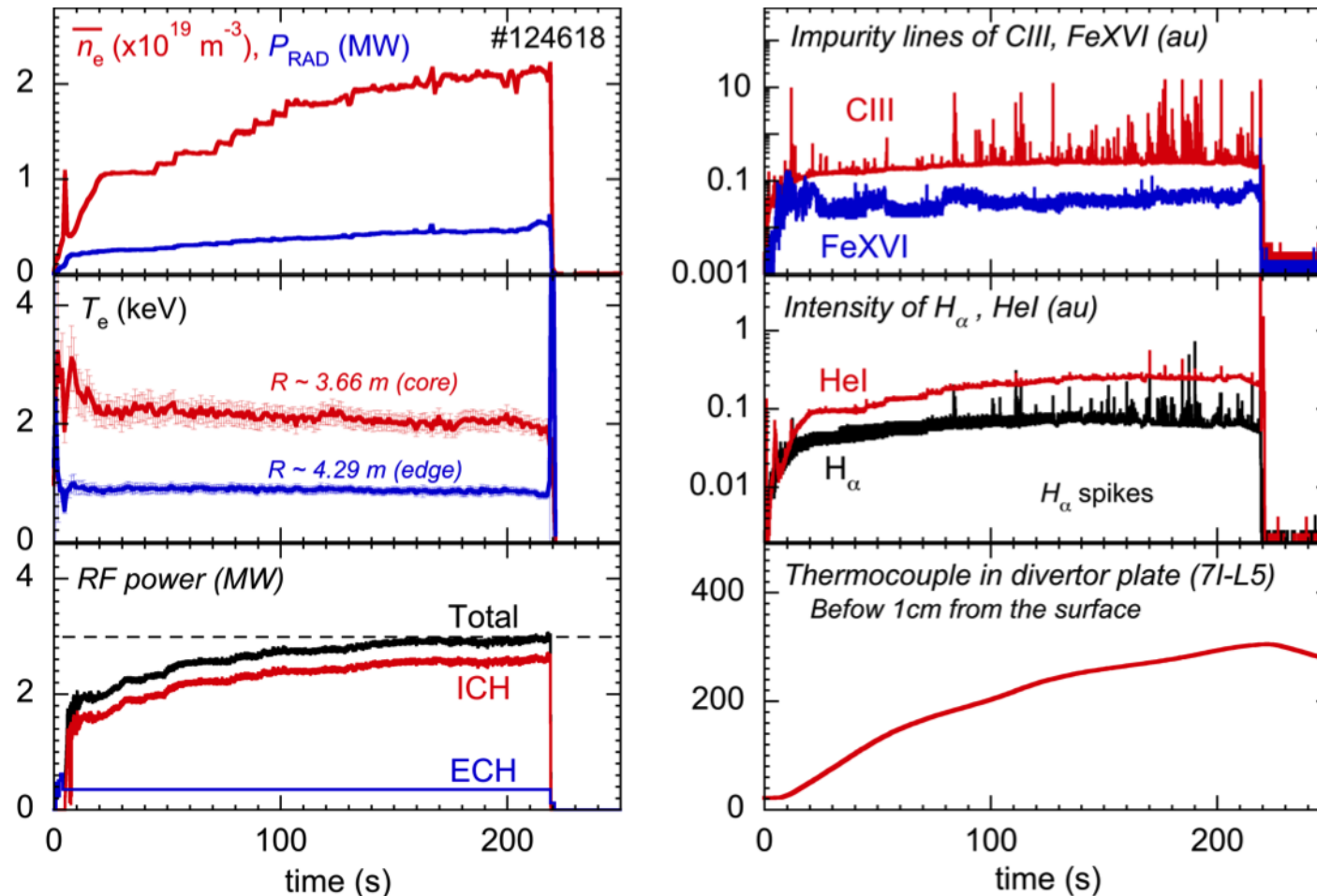
Particle cohesion of He bubbles

Physical prosperity of MMLs
Dense, hard, and brittle

First trial of the high-power steady-state heating (2-3MW) with the design value of the LHD

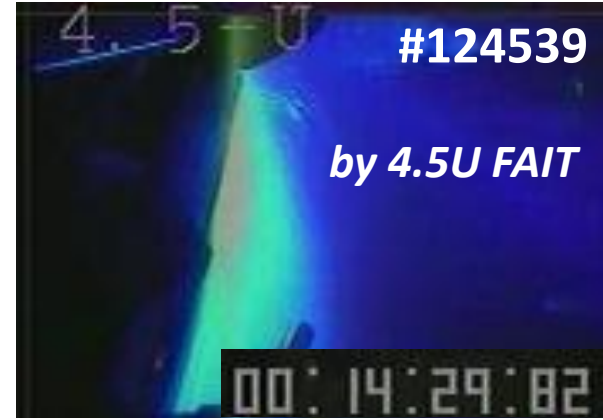
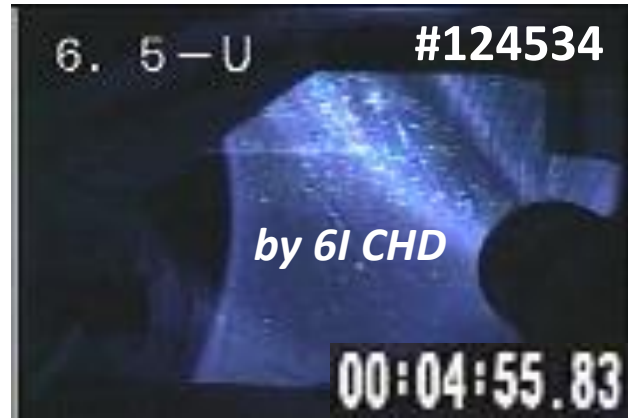
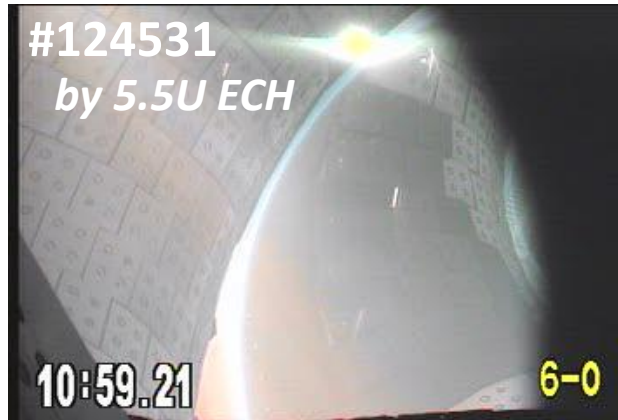


Command values of RF heating power and electron density were manually increased after confirming the health of heating devices and LHD devices.



The clear correlation between H_α and CIII was first observed, and it played the key role for understanding the sudden impurity entrance.

Collections of plasma collapse with the high-power steady-state heating



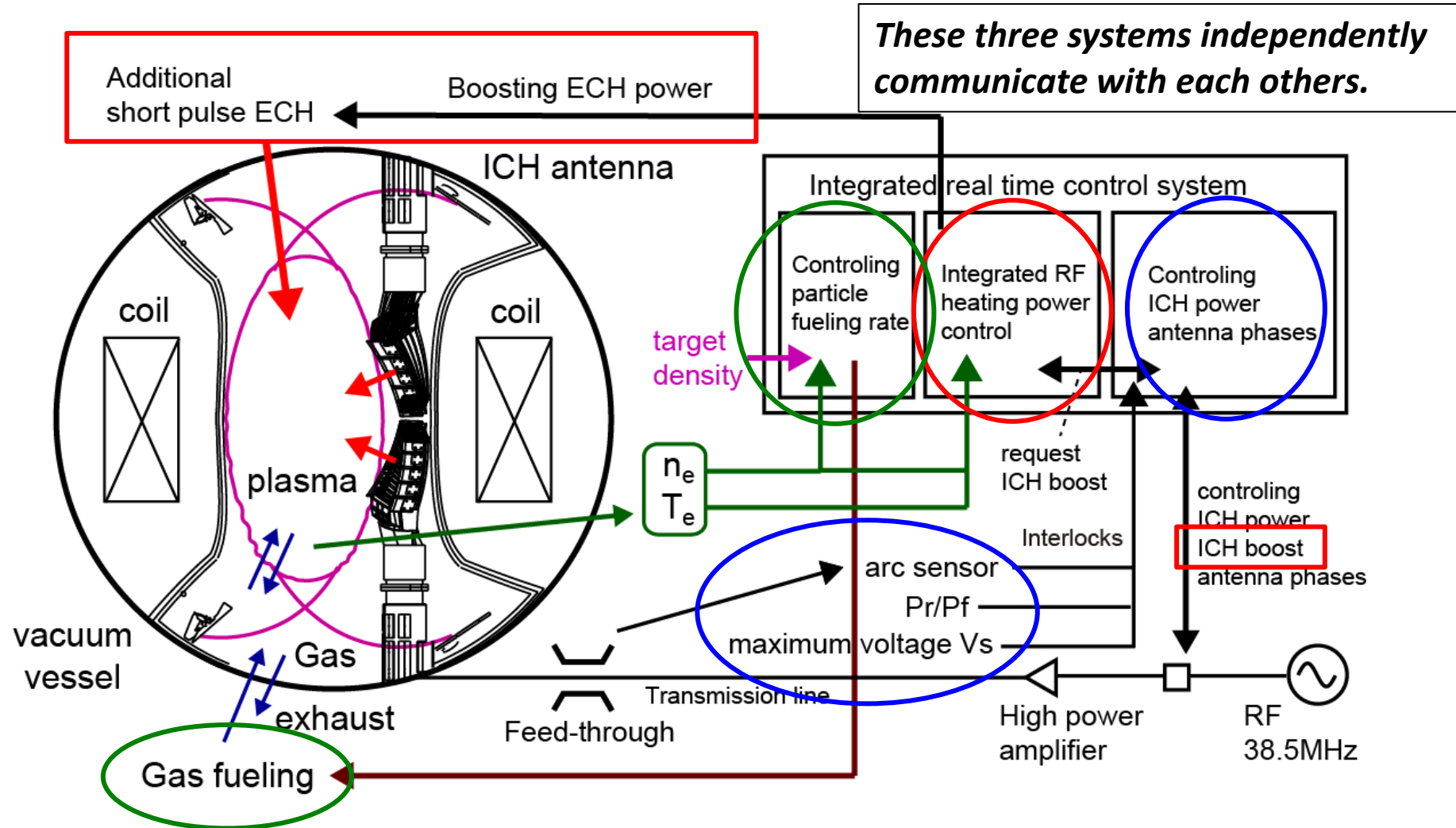
The causes of plasma collapses in the long-pulse discharges were not oriented to particular reasons, but **a large amount of impurity mixing occurred to degrade the health of plasma. (Temperature degradation is critical to maintain the plasma.)**

An integration of RF heating systems and density-control relieves critical perturbations of plasma duration.



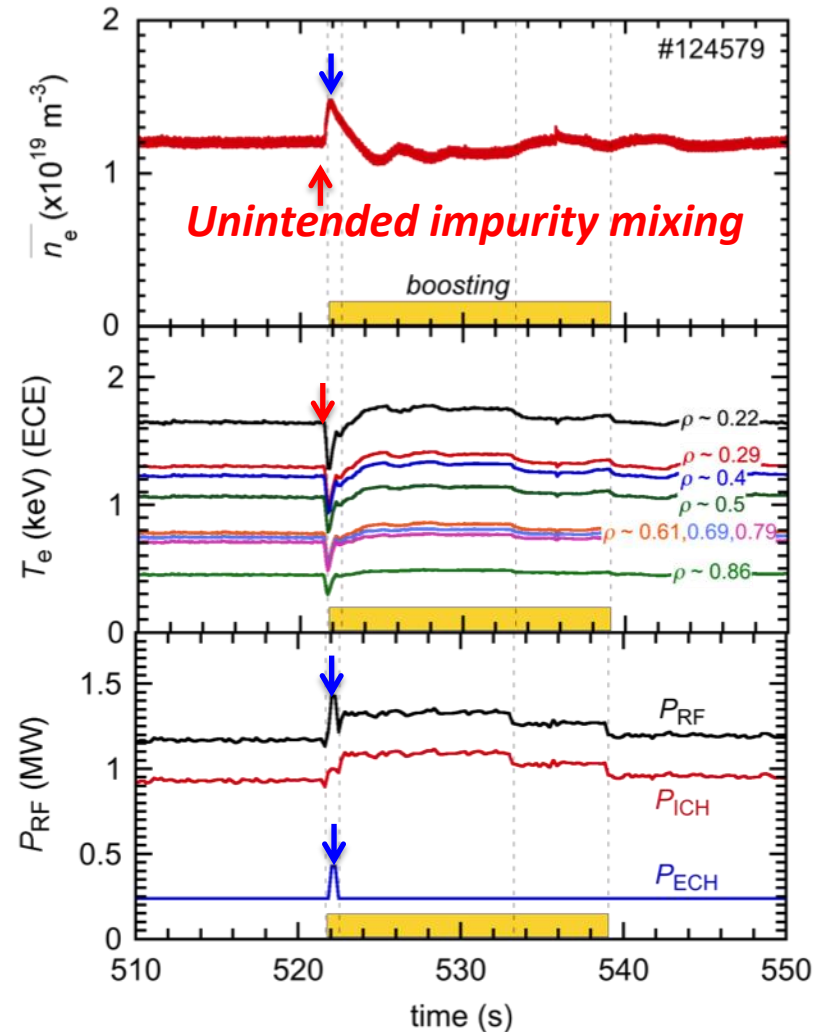
Critical time-scales of plasma collapse are less than 0.2 sec ($\sim \tau_E$).

Automatic recovery scheme is required for the stable long-pulse plasma duration.



The integrating RF heating systems and the gas-fueling control relieved plasma perturbations for density and temperature in a few seconds.

The boost of RF heating power worked to effectively maintain the plasma parameters.



A unintended event occurred at $t \sim 522$ sec, and boosting RF heating power was carried out at the short-time delay ($< \text{ms}$).

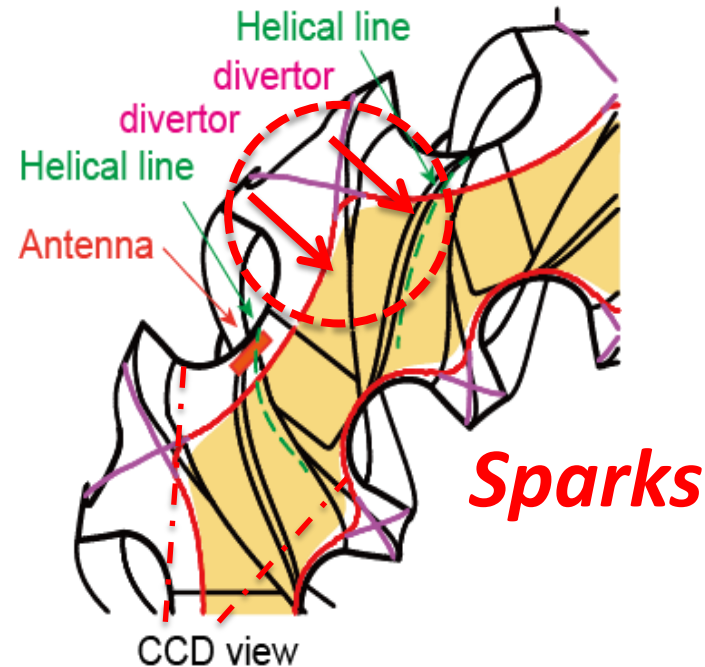
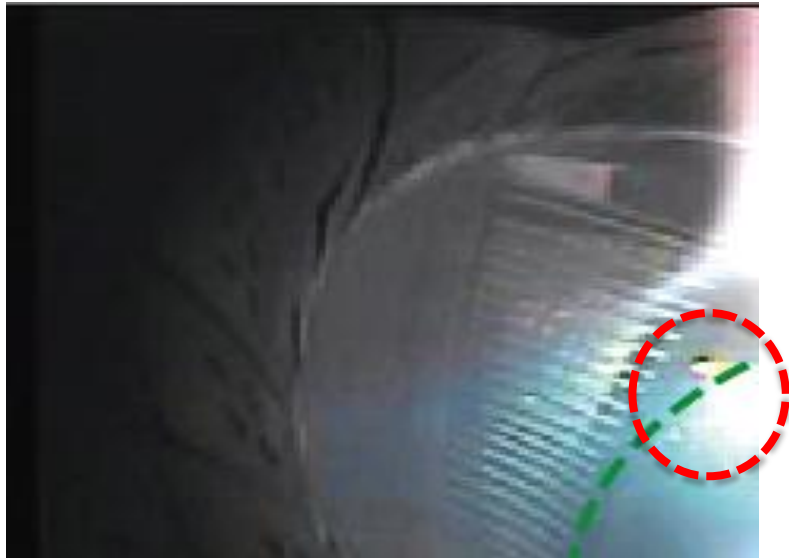
By boosting RF power, plasma density and temperature was recovered to the similar levels just before the event, and robust plasma with the ultra-long pulse and higher performance was demonstrated by these developments in the LHD.

However, the next critical issue of breaking steady-state plasma appeared...

Strong sparks were mitigated by continuous hydrogen fueling.



When the plasma duration was extended, sparks were easily observed at the neighboring port of the PA antenna.

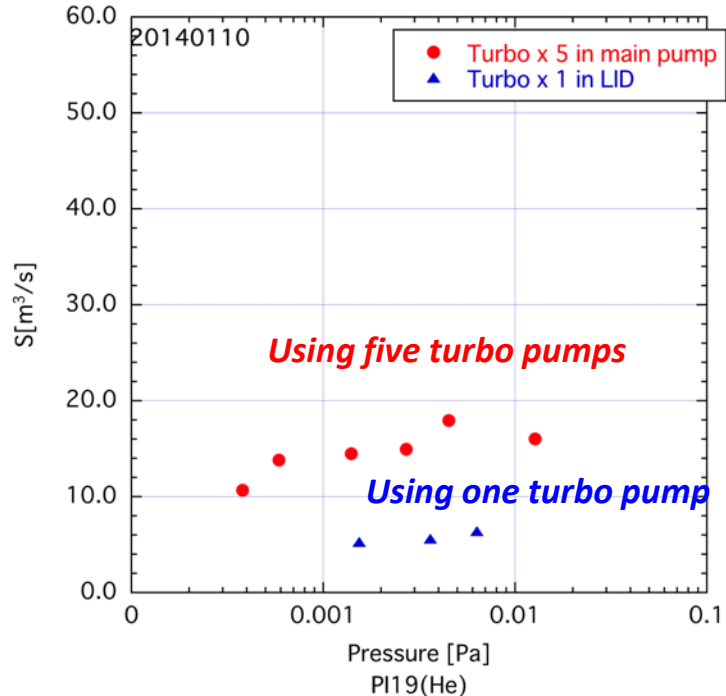


Fueling hydrogen effectively mitigated strong sparks around the PA antenna, but several minutes elapsed until the mitigation of sparks. For the RF heated steady-state operations, the long-pulse discharges strongly decreased the wall-recycling rate, this caused the degradation of actual hydrogen fueling to the plasma. (It needs time to increase the hydrogen minority ratio inside the plasma.)

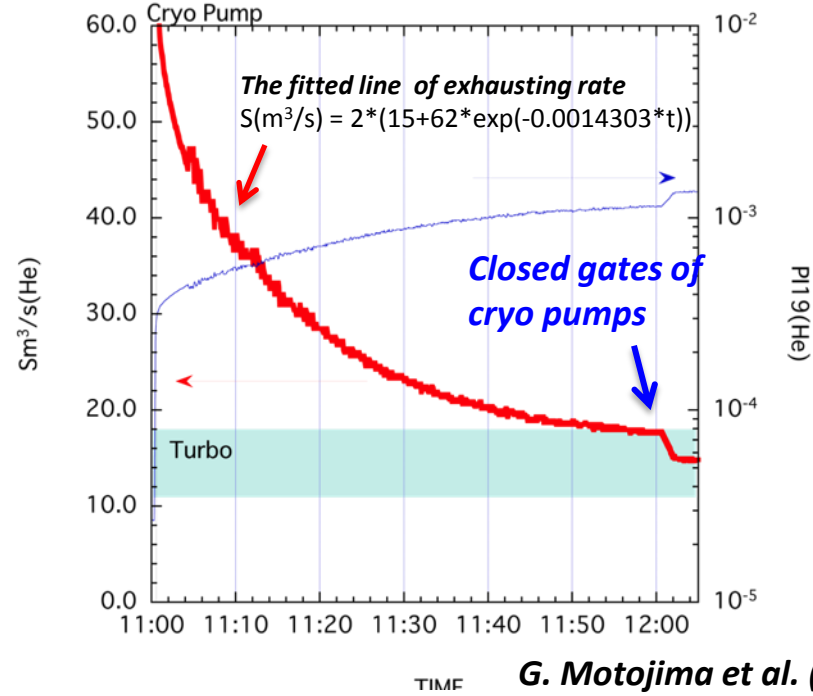
Confirming the exhausting ability of He particles using the cryo-absorption pump



Only turbo molecular pump

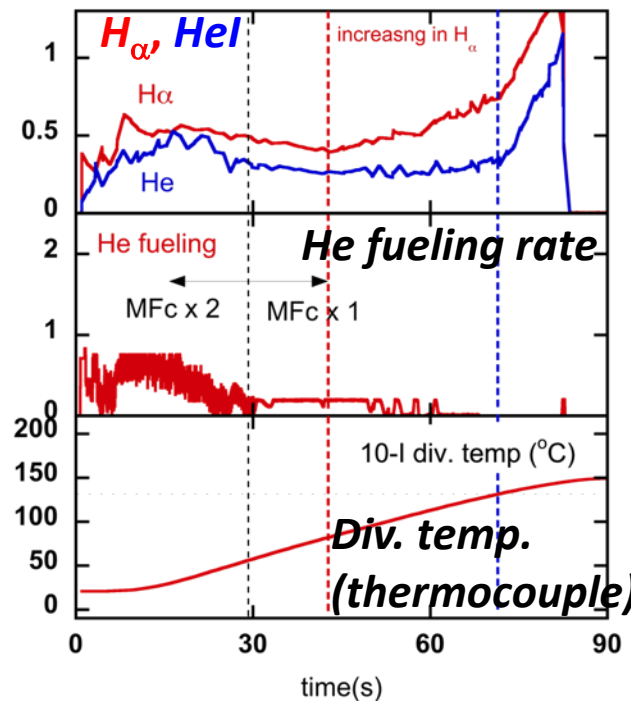
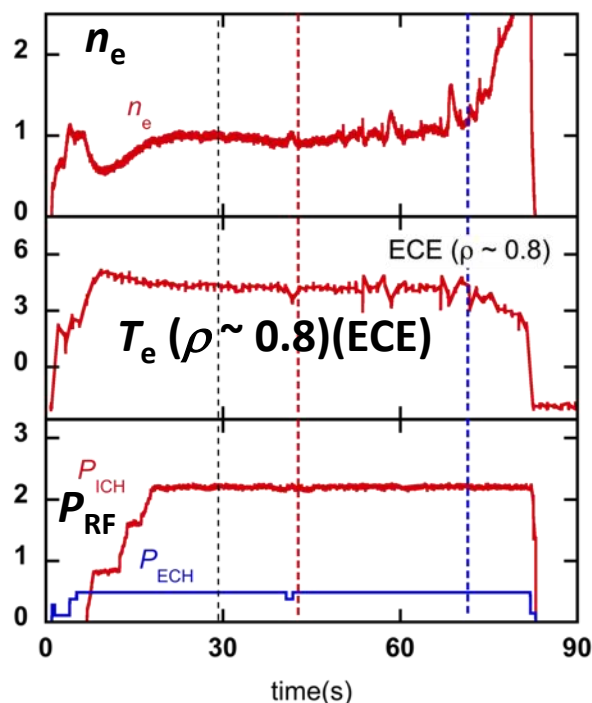


Ten cryo-absorption pump and five turbo pumps

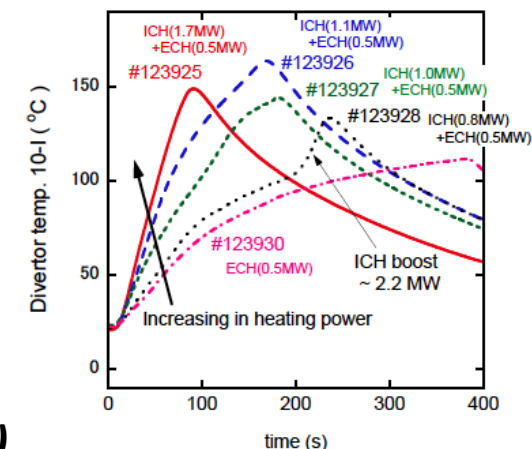


The exhausting ability of He particles using the turbo-molecular pump is approximately $16 \sim 19 \text{ m}^3/\text{s}$ in the surrounding pressure of $10^{-2} \sim 10^{-3} \text{ Pa}$. The exhausting ability using the cryo-absorption pump was not negligible after the particle desorption. After continuous He fueling (\sim one hour), the active exhausting rate of the cryo pump will be small ($\sim 4 \text{ m}^3/\text{s}$), and it is necessary to consider the time evolution of the fueled he particles.

Desorption gas from divertor plates shortened plasma duration time when the heating power was increased.

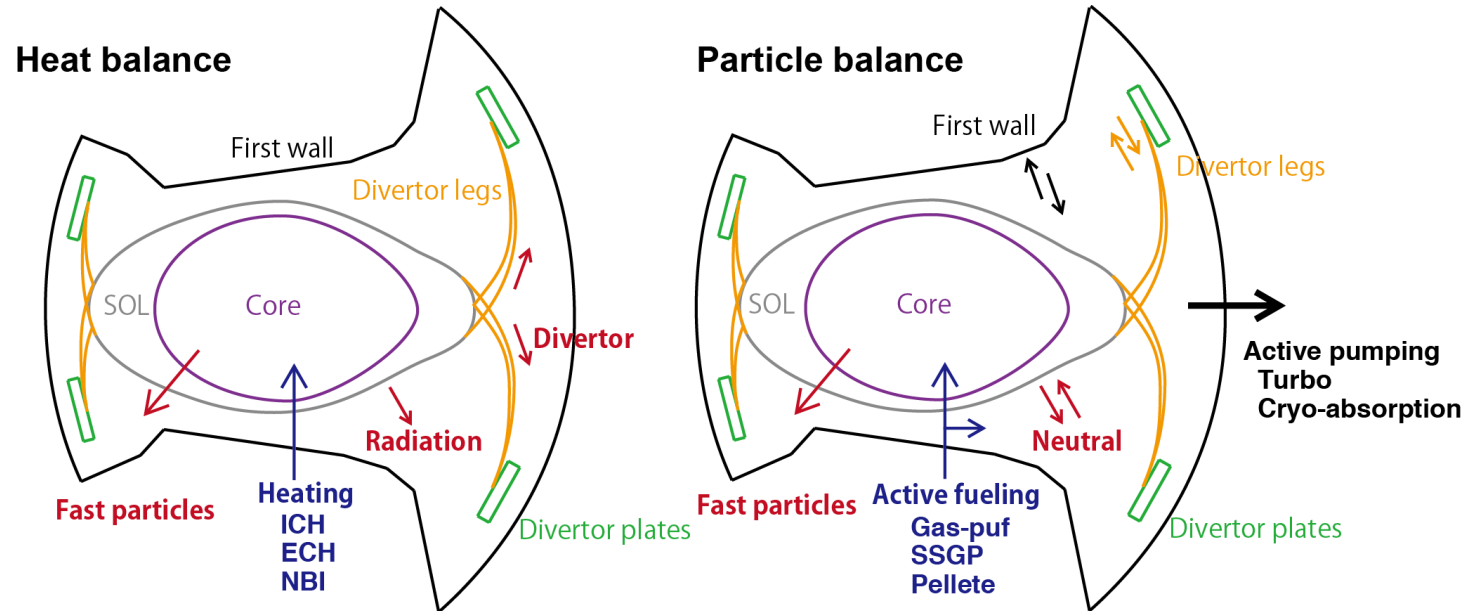


***Reversed magnetic field configuration**



- The intensity of the H_{α} spectrum was increased after 40 sec, and H_{α} and the HeI line was rapidly rose at 70 sec.
- After 30 sec, He fueling was stopped while keeping density constant, and the desorption of He particles seemed to occur around the divertor plates because the difference between at $t \sim 0$ sec and at $t \sim 70$ sec for first wall temperature was negligible.
- When increasing heating power, the clear start time of desorption was shortened, and gas desorption from the divertor plates was necessary to maintain plasma duration.

Heat and particle balances on the steady-state operation



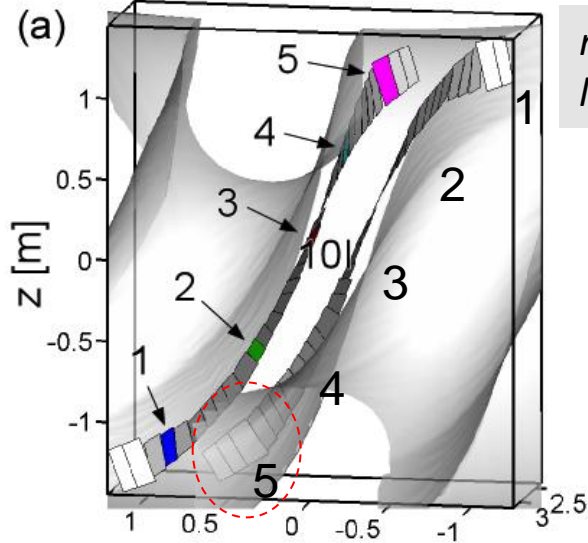
- Heat balance is easily estimated by the heating source and by removing off power of cooling water on SSO:

$$\text{Heating } (P_{RF}) = \text{Radiation } (P_{rad}) + \text{Divertor } (P_{div}) + \text{Wall } (P_{other}) \text{ (fast + protector + heating loss)}, P_{rad} \sim 17\%, P_{div} \sim 56\%, P_{other} \sim 27\% \text{ (\#124579, } P_{rad} \sim 1.2\text{MW)}$$

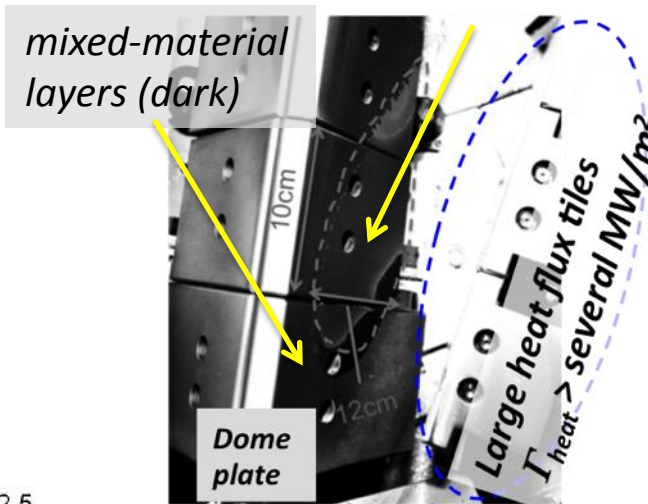
- Retention rates (desorption and absorption) for wall and divertor are functions of the surface temperatures and surrounding pressure. On the SSO with thermal equilibrium, the various temperature profiles for toroidal, poloidal, and heating geometrical conditions make more complicated estimation of the retention rates.

One of the carbon sources is a carbon-rich mixed-material layer around divertor tiles, and the thickness of the layer was extended during continuous SSO.

Closed helical divertor w/o dome plates



Exfoliated carbon-rich mixed-material layer



The history of a mixed-material layer and the elements

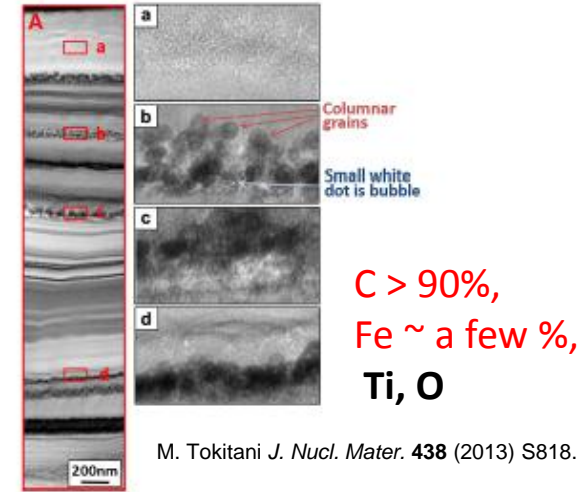
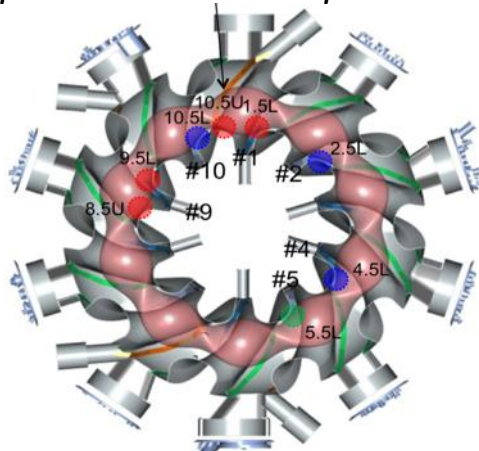


Fig. 3. Right series (a-d): High resolution TEM micrographs corresponding to the small frames in (A).

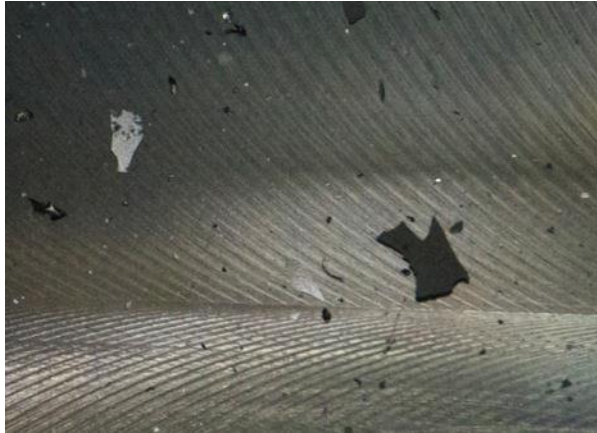
Thick mixed-material layer was observed around particular divertor plates.



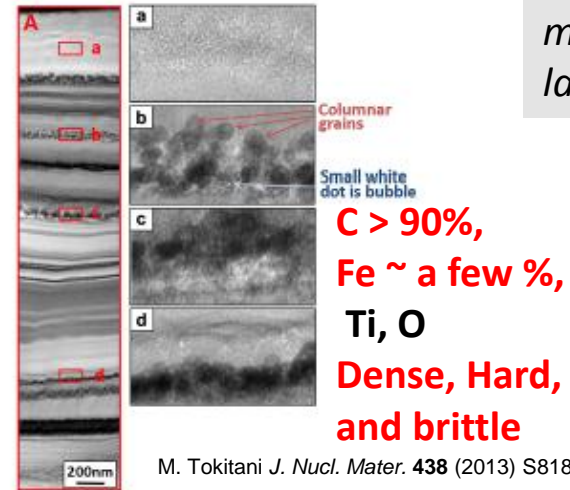
- Mixed-material layer strongly grew around the particular divertor plates with the large heat flux and the geometrically dense region.
- The main elements of the mixed-material layer were C (>90%) and Fe (~ a few %), and the layer effectively grew in continuous divertor erosion.
- The layer is dense, hard, and brittle, and the thick layer is easily exfoliated by the heat stress and the bubble of trapped particles (He and/or H).

One of the carbon sources is a carbon-rich mixed-material layer around the divertor tiles, and the thickness of the layer was extended during continuous SSO.

Small flakes are on the port far from the plasma (center ~ 3m).



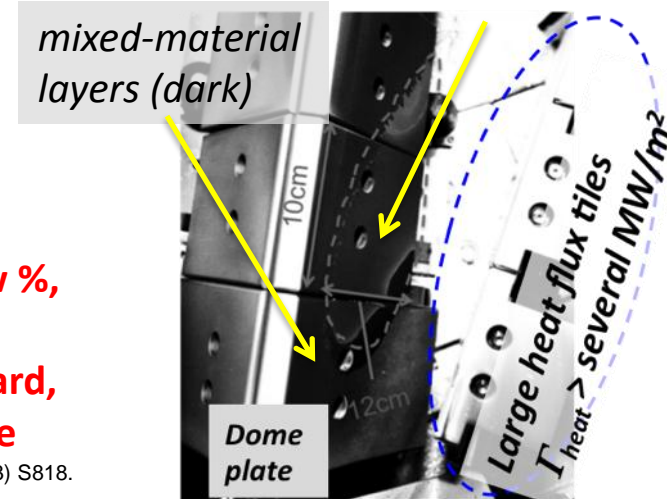
The history of a mixed-material layer and the elements



M. Tokitani *J. Nucl. Mater.* **438** (2013) S818.

Fig. 3. Right series (a-d): High resolution TEM micrographs corresponding to the small frames in (A).

Exfoliated carbon-rich mixed-material layer

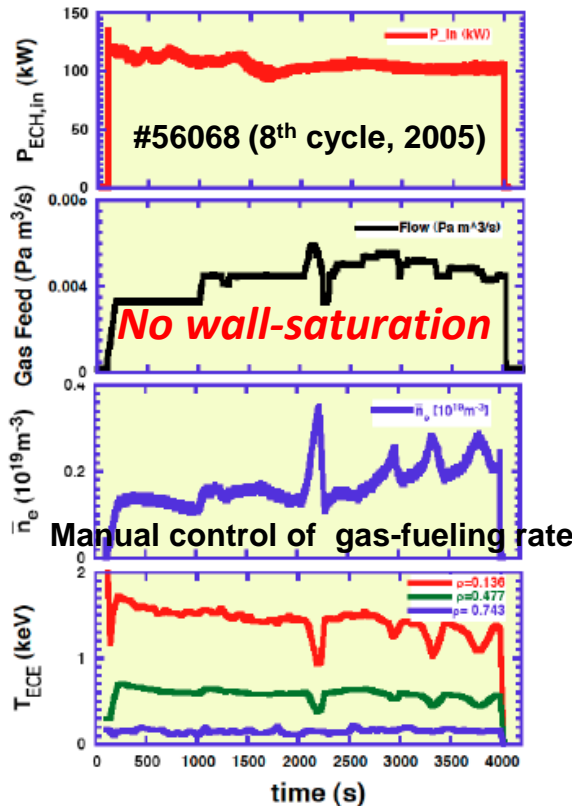


- *As high-power plasma duration time with the increase of heating power was extended, small flakes and carbon-rich mixed-material layer (MML) were observed everywhere.*
- *The main elements of the flakes were carbon (>90%) and iron (~ a few %), and the thicknesses of MML grew around the particular divertor plates with the large heat flux and the geometrical dense region.*
- *The ultra-long pulse plasma was collapsed by the continuously exfoliated MMLs with the large region (~ 10 cm x 12 cm). This will be a critical new issue.*

Typically early long-pulse plasma discharges in the LHD



2nd harmonics ECH (84GHz) (3900s)
 $B=1.48\text{T}$, $R_{ax} \sim 3.53\text{m}$, $P_{in} \sim 0.1\text{MW}$

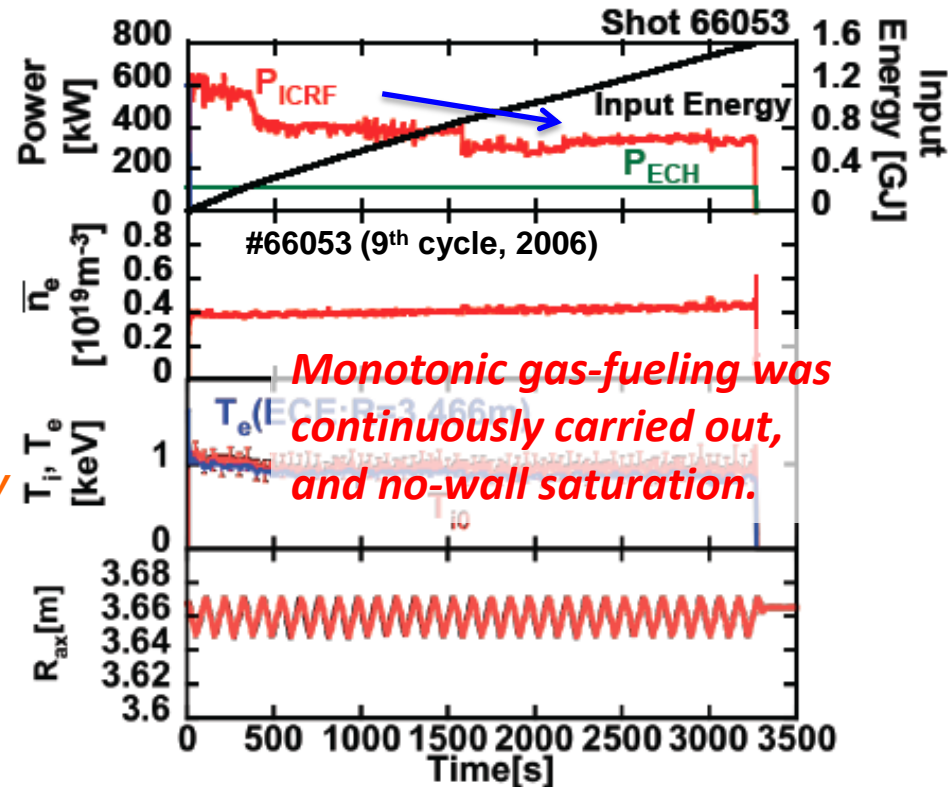


Manual control of gas-fueling rate



Increasing the heating power and plasma density

ICH+ECH (38.5MHz, 84GHz) (3268s)
 $B=2.71\text{T}$, $R_{ax} \sim 3.64\text{-}3.67\text{m}$, $P_{in} \sim 0.5\text{MW}$

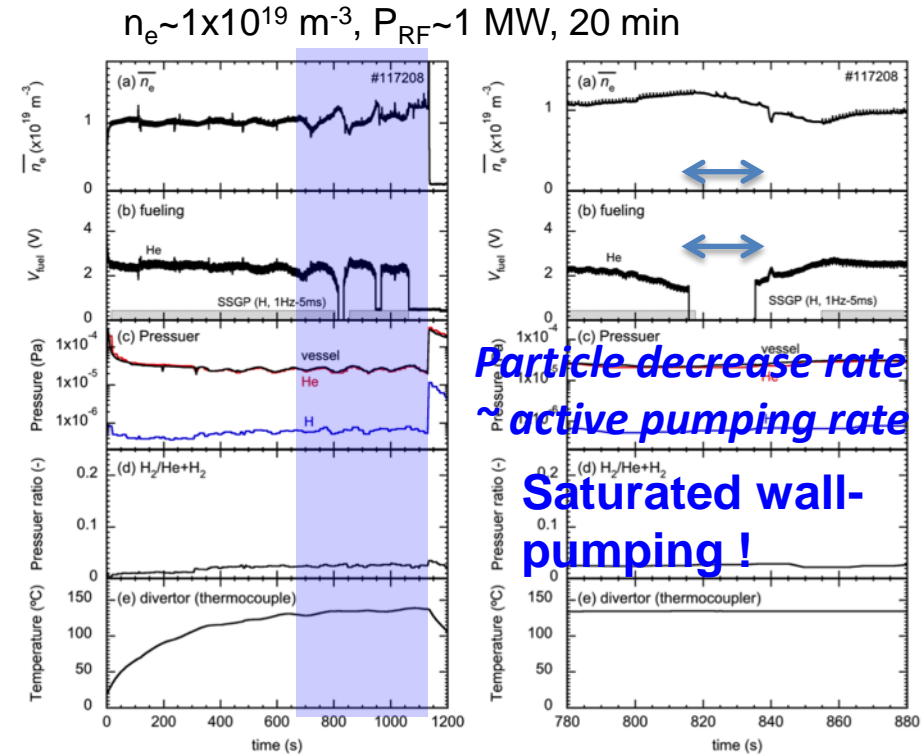
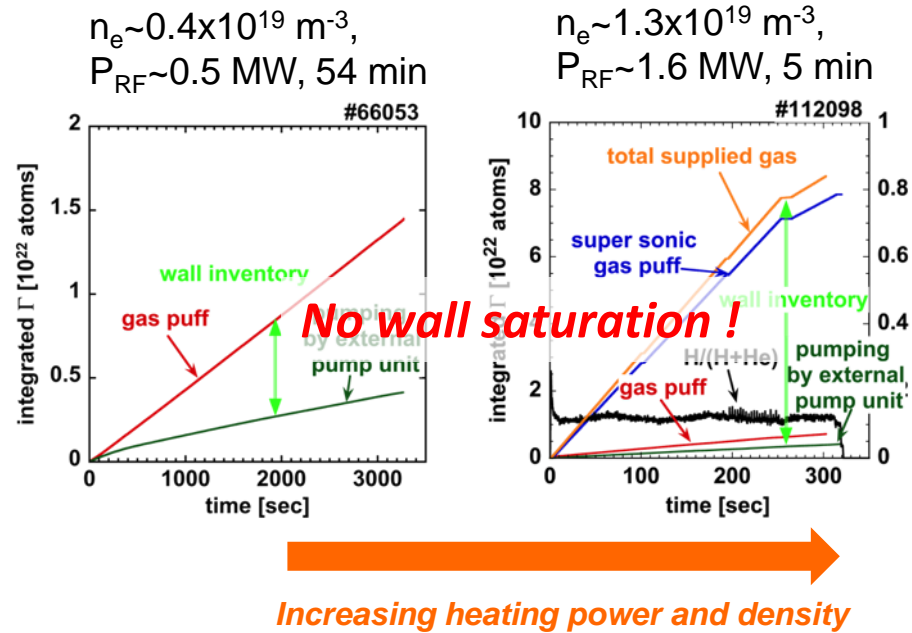


Monotonic gas-fueling was continuously carried out, and no-wall saturation.

- Particle fueling continuously occurs, and the wall-pumping has been active for the He plasma. (Not steady-state conditions for PWI)
- In order to mitigate sparks, heating power must be decreased because the sparks are one of the impurity mixing sources. This is a critical issue for high performance plasma discharge.

Density control lapsed into difficulty in the several ten minutes plasma discharge with $P \sim 1\text{MW}$ and $n_e \sim 10^{19}\text{ m}^{-3}$.

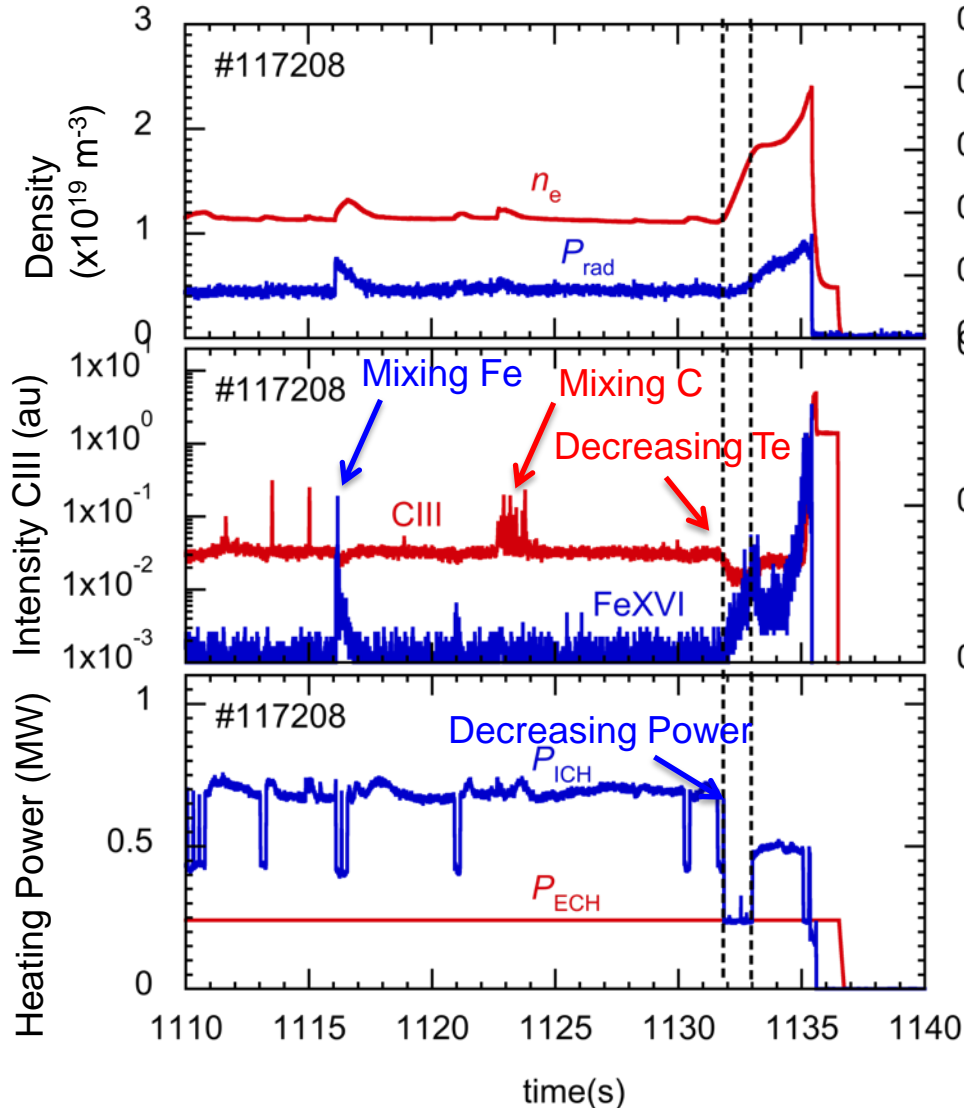
For keeping steady-state ICH, minority-ratio control is an important issue, and the controls of density and neutral gas-pressure are necessary to extend plasma duration.



After 700 sec with the density of $1 \times 10^{19}\text{ m}^{-3}$ and heating power of 1 MW, the wall-pumping seemed to be first negligible and uncontrollable using early gas-feedback system. (Needs improvement of the gas-fueling system)

One of the critical issues for collapsing the long-pulse plasma with $T_e \sim 2\text{keV}$ and $P_{RF} \sim 1\text{ MW}$ was caused by the degrading heating power.

Time evolution of the plasma collapse for early long-pulse discharge with $P_{RF} \sim 1\text{ MW}$ and $n_e \sim 10^{19}\text{ m}^{-3}$



A chart of the collapse for steady-state plasma durations

Decreasing heating power

$T_e, T_i \downarrow$

There is no additional heating support, and then ...

Increasing the amount of the intensities or impurity lines (FeXVI, CIII)

$n_e \uparrow$

Failing the control of density keeping, and then ...

Increasing the density and the radiation

Unstable

The health of the plasma is extremely weakens, and then ...

Plasma collapse

$P_{rad}/P_{RF} > 40\%$. Impurity mixing easily occurs with the low temperature.



- *The extension of steady-state plasma duration with MW-class heating, and the operation regions*
- *Result of ultra-long pulse plasma duration with $\tau_d \sim 48$ min, $P_{RF} \sim 1.2$ MW, $n_e \sim 1.2 \times 10^{19} \text{ m}^{-3}$, $T_e \sim T_i \sim 2$ keV, and $W_{inj} \sim 3.4$ GJ*
 - *Thermal behavior and typical temperatures*
 - Inhomogeneity of divertor heat flux*
 - *The steady-state was terminated by sudden unintended entrance of the exfoliated mixed-material layers (MMLs) with continuous divertor erosion*
 - *Characteristics of the MMLs*
 - Thick region, the growth rate, the main elements, the physical property, and the trappable ability of He particles*
 - *Preliminary estimation of He particle balance with the MMLs*
- *Summary and future plans*